

M-Pos483

KINETIC PROPERTIES OF THE VOLTAGE DEPENDENT HUMAN DELAYED RECTIFIER CHANNEL h-DRK1

((R. Koopmann¹, K. Benndorf^{1*}, C. Lörz² and O. Pongs²)) ¹Institut für Vegetative Physiologie, Universität zu Köln, 50924 Köln. ²Zentrum für molekulare Neurobiologie, Martinstr. 52, 20251 Hamburg. *Heisenberg-fellow of the Deutsche Forschungsgemeinschaft. (Spon. by P. Honerjäger)

The gene of the human delayed rectifier K⁺ channel h-DRK1 was cloned and the channels were expressed in *Xenopus* oocytes. Whole cell currents at various potassium concentrations were measured with the two electrode voltage clamp technique. The currents activate at potentials positive to -20 mV and are shown to be highly selective for K⁺ ions. Using the patch clamp technique macroscopic currents (macro-patches or giant patches) and single channel currents (micropatches) were measured (5.4 mmol [K⁺]_o). In giant patches, ionic and putative on- and off-gating currents were recorded simultaneously. It is estimated that less than 1% of the gating channels actually opened. In tail currents the putative off-gating current was separated from the ionic current by different kinetics. The instantaneous current-voltage relationship rectified outwardly to a higher degree than predicted by the Goldman-Hodgkin-Katz equation. Using a sequential Markovian model with four independent voltage controlled transitions, voltage dependence of the open probability could only be explained by assuming at least two components of activation. In the single channel activity, sublevel openings could be observed regularly but a main level with a unitary conductance of 9.4 pS (0 to +80 mV) was present. The open time was distributed biexponentially with voltage independent time constants in the range of 1 and 10 ms (filter 1 kHz). The time courses of cumulative first latency and ensemble averaged currents in single channel patches suggested that even a single channel may operate with two different components of activation.

ENERGY TRANSDUCTION

M-Pos485

THYROID HORMONES INDUCE Mg²⁺ RELEASE FROM ISOLATED RAT CARDIAC AND LIVER MITOCHONDRIA THROUGH THE ACTIVATION OF THE PERMEABILITY TRANSITION PORE.

A. Romani, C. Marfella and M. Lakshmanan^{*} Dept. s Physiology & Biophysics and Medicine, Case Western Reserve University, Cleveland, OH, 44106, USA. (Spon. by T. Hoshiko).

Recently we provided evidence that the activation of mitochondrial adenine nucleotide translocase (AdNT) by cAMP induced the extrusion of a sizeable amount of Mg²⁺ from cardiac or liver mitochondria. Since it has been proposed that AdNT may represent a target for I₃ as well, the possibility that thyroid hormones may also induce a similar Mg²⁺ efflux from mitochondria was investigated. The addition of 5 pM T₃ or 10 pM T₄ to isolated cardiac or liver mitochondria prompted a release of approx. 2-3 nmol Mg²⁺/mg protein from both mitochondria preparations. This efflux, which was quantitatively similar to that induced by cAMP stimulation, could also be induced by other thyroid hormone analogs, such as TRIAC, r-T₃, 3,3',5'-T₂, L94901 and 3,5-T₂. When these experiments were performed in the presence of 100 μM atracyloside, a specific inhibitor of AdNT, only the efflux induced by cAMP was prevented while the thyroid hormone mediated Mg²⁺ extrusion was unaffected. HPLC measurements of mitochondrial ATP content showed a decrease in ATP content following the stimulation by cAMP. This decrease correlated well with the amount of Mg²⁺ extruded under the same experimental conditions. In contrast, an increase in ATP content was observed following the stimulation by T₃. When these experiments were repeated in the presence of 1 μM cyclosporine-A, a specific inhibitor of the mitochondrial permeability transition pore (PTP), the Mg²⁺ efflux induced by T₃ was completely blocked. These data indicate that the stimulation of cardiac and liver mitochondria by thyroid hormone induces a major efflux of Mg²⁺ from mitochondria, which may have regulatory effects on mitochondrial metabolism. This efflux appears to occur through the opening of PTP. (Grants N.I.H. 1K08DK01870 & N.I.H. HL 18708).

M-Pos487

EFFECT OF SUBSTRATE ON NADH LEVELS OF OXYGENATED, ISOLATED VENTRICULAR MYOCYTES DURING ELECTRICAL PACING ((RL White[†] & BA Wittenberg[‡])) [†]Temple University Medical School, Philadelphia, PA 19140 & [‡]Albert Einstein College of Medicine, Bronx, NY 10461.

Mitochondrial NAD(P)H levels were measured using endogenous microfluorescence of single cells freshly isolated from rat heart. The NAD(P)H level was determined from the emitted fluorescence at 415 nm and 455 nm during brief epillumination at 365 nm. Cells were electrically paced by Pt-Ir field electrodes and superfused with MEM containing glucose and equilibrated with 95% O₂ and 5% CO₂ for the duration of the experiment. The fraction of reduced NAD[P], (NADH) was 0.41±0.04 (n=5) in myocytes contracting at 0.5 Hz for 20 min. When pacing was increased to 5 Hz for 10 minutes NADH decreased reversibly to 0.29±0.04 (n=5), and oxygen uptake increased 5-fold. At this stimulation rate, measured pH_i remained constant and [Ca⁺⁺]_i is known to increase. NADH recovered to control values after 20 min. at 0.5 Hz. Similar results were obtained when MEM containing glucose was supplemented with palmitate, octanoate, or β-OH butyrate. In contrast, NADH remained essentially unchanged during stimulation when cells were superfused with MEM containing glucose supplemented with lactate, pyruvate, or α-ketoglutarate. Pyruvate enhances the activity of the mitochondrial pyruvate dehydrogenase and maintains high NADH during pacing. This suggests that increased [Ca⁺⁺]_i does not maximally stimulate the rates of mitochondrial α-ketoglutarate or pyruvate dehydrogenases during increased pacing. Under these conditions, substrate supply to the dehydrogenases may be limiting. We conclude that during electrical pacing sufficient to increase oxygen consumption 5-fold, the reduction in NADH levels may reflect a drop in mitochondrial protonmotive force when dehydrogenase reaction rates are submaximal.

M-Pos484

FUNCTIONAL DOMAINS IN THE AMINO-TERMINAL REGION OF MAMMALIAN NEURONAL I_{K(A)} CHANNELS.

((H. Ehmke, M. Koenen, J. Siara, J.P. Ruppersberg)). Max-Planck-Institut für Medizinische Forschung, Jahnstraße 29, 69120 Heidelberg, Germany (Spon. by L. Wollmuth).

Studies on *Shaker B* K⁺ channels have implicated two major functional domains located in the amino-terminal region: a sequence comprising the first 20 amino acids which mediates fast inactivation (Hoshi et al., Science 250:533-38, 1990), and a hydrophilic sequence of 114 amino acids which appears to be essential for subunit assembly (Li et al., Science 257:1225-30, 1992). We have examined whether these structure-function relationships also exist in a homologous mammalian voltage-dependent K⁺ channel. Mouse Kv1.4 channels were expressed in *Xenopus* oocytes and macroscopic currents were obtained in the cell-attached and inside-out configuration. Surprisingly, deletion of the first 37 amino acids (ball-region) did not slow but even accelerated inactivation. Larger amino-terminal deletions, however, resulted in a loss of fast inactivation, while it was preserved in channels with internal deletions leaving the ball-region intact. Cytoplasmic application of the pore blocker TEA slowed inactivation in the wild type but not in the amino-terminal mutations. Expression of functional channels was still obtained when the amino-terminal deletion included most of the hydrophilic assembly site. These data 1) demonstrate the presence of a ball-and-chain inactivation gate in mammalian neuronal K⁺ channels, but 2) argue against a functionally important assembly domain in the amino-terminal region.

M-Pos486

ATPase ACTIVITY, IF1 CONTENT AND PROTON CONDUCTIVITY OF ESMP FROM CONTROL AND ISCHEMIC SLOW AND FAST HEART-RATE HEARTS. ((W. Rouslin, C.W. Broge, F. Guerrieri and G. Capozza)) Department of Pharmacology and Cell Biophysics, Univ. of Cincinnati Col. of Medicine, Cincinnati, Ohio, USA and Inst. of Medical Biochemistry and Chemistry, Univ. of Bari, Bari, Italy.

Slow heart-rate hearts have heart rates of approx. 200 beats/min or less and contain predominantly the slow myosin ATPase isoform. Fast heart-rate hearts are capable of heart rates of approx. 300 beats/min or more and contain predominantly the fast myosin ATPase isoform. Earlier studies by us showed that slow heart-rate hearts exhibit a marked IF1-mediated inhibition of the mitochondrial ATPase during ischemia whereas fast heart-rate hearts do not. In the present study we used rabbit as the slow heart-rate species and rat as the fast heart-rate species. Rat is a fast heart-rate species that contains a low level of IF1. When sonicated at pH 8.0 with 2 mM EDTA, control rat heart ESMP exhibited approx. the same oligomycin-sensitive ATPase activity as control rabbit heart ESMP, but somewhat less than half the IF1 content and approx. twice the oligomycin-sensitive proton conductivity of control rabbit heart ESMP. In the same experiments, ischemic rabbit heart ESMP exhibited approx. 27% lower oligomycin-sensitive ATPase activity, approx. 1.5 IU/mg more IF1 and approx. 23% lower oligomycin-sensitive proton conductivity than control rabbit heart ESMP whereas ischemic rat heart ESMP exhibited only nominally lower ATPase activity, approx. 0.02 IU/mg more IF1 and unchanged oligomycin-sensitive proton conductivity compared to control rat heart ESMP. (This work was supported by NIH grant HL30926).

M-Pos488

EFFECTS OF THE CREATINE ANALOGUE β-GUANIDINOPROPIONIC ACID ON PORCINE CAROTID ARTERIES USING ³¹P NMR.

((E. A. Boehm, J. F. Clark and G. K. Radda)) Department of Biochemistry, University of Oxford, Oxford, OX1 3QU.

The responses of phosphocreatine and ATP as energy intermediates in vascular smooth muscle have been investigated by studying the acute energetic effects of the creatine analogue β-guanidinopropionic acid (β-GPA) on porcine carotid arteries using ³¹P NMR. β-GPA enters the smooth muscle cells, where it is phosphorylated by creatine kinase to produce β-GPA-P.

Fresh porcine carotid arteries were collected at the abattoir and kept cold till the experiments began. The tissue was superfused for 12 hours with Krebs-Henseleit buffer at 22°C, containing NaCl substituted β-GPA (50 mM), and either glucose (10 mM) or pyruvate (5 mM) as substrate. Perfusion without β-GPA was used as a control system. Tissues were subsequently frozen in liquid nitrogen, for [metabolite] analysis.

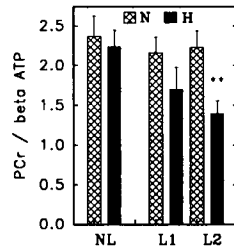
Perfusion with β-GPA led to the formation of observable β-GPA-P after an initial lag period of about 2 hours with a concomitant decrease in [PCr]. The rate of β-GPA phosphorylation was significantly greater when glucose was used as substrate. Accumulation of β-GPA-P was accompanied by significant decreases in both tissue [lactate] and [ATP]. We hypothesise that increased ATP utilisation due to the presence of an additional phosphorylatable compound leads to a lower [ATP] which may stimulate oxidative metabolism (via increased [ADP]), with a concomitant decrease in tissue [lactate].

We conclude that the rate of β-GPA phosphorylation is greater with glucose as substrate as compared with pyruvate. Vascular smooth muscle (a glycolytic tissue) has a greater [ATP] when perfused with glucose. We believe that the greater [ATP] may enable a more rapid phosphorylation of β-GPA.

M-Pos489

DEPRESSION OF PHOSPHOCREATINE STORES IN ISOMETRICALLY CONTRACTING HYPERTROPHIED FAILING GUINEA PIG HEARTS.
(L.A. Jelicks and F.M. Sirl) Albert Einstein College of Medicine, Bronx, N.Y.

The potential involvement of altered myocardial energetics in the pathophysiology of heart failure has been controversial, in part due to frequent reports of normal ATP and/or phosphocreatine (PCr) levels in hearts with known functional impairment. The hypothesis that these high energy phosphate stores of hypertrophied failing hearts are more labile than those of normal hearts following imposition of isometric workload was tested by ^{31}P -NMR spectroscopy in isolated Langendorff-perfused hearts from normal (N) and hypertrophied failing (gradual ascending aortic banding; H) guinea pigs. Five hearts from each group were examined under unloaded conditions (NL), and another 5 from each group were examined while contracting isometrically against a balloon filled such that either moderate (approx. 50 mm Hg; L1) or high (approx. 100 mm Hg; L2) left ventricular developed pressures were achieved. There were no significant differences between N and H in either pH (for NL, N: 7.13 ± 0.13 ; H: 7.10 ± 0.14 means \pm SD) or phosphorylation potential (for NL, N: 13.4 ± 1.6 ; H: 12.5 ± 1.9 in units) under any conditions (NL, L1, L2) whereas PCr was significantly depressed only in H at L2 (Figure: means \pm SE; **, $P < 0.02$), suggesting a diminished capacity of those hearts to maintain PCr stores at high physiologic workload



M-Pos491

OXONOL V IN BEEF HEART SUBMITOCHONDRIAL PARTICLES: SEPARATION OF FLUORESCENCE FROM SURFACE POTENTIALS, DIFFUSION POTENTIALS, AND ENERGIZATION. ((J.C. Freedman, T.S. Novak, H.S. Penefsky and W.D. Stein)) SUNY Health Sci. Ctr., Syracuse NY 13210

With beef heart submitochondrial particles the fluorescence of the anionic dye Ox V (bis[3-phenyl-5-oxoisoxazol-4-yl]penta-methineoxonol) increases in response to inside positive diffusion potentials induced by gramicidin at nMolar dye, but decreases at μ Molar dye. Upon energization with succinate or ATP (also giving inside positive transmembrane voltages), dye fluorescence increases at low [membrane] with nMolar dye, but decreases at μ Molar dye. Decreases in fluorescence at μ Molar dye accompany energization of mitochondria and of submitochondrial particles, despite opposite polarity of their transmembrane voltage, confirmed by flow dialysis. Decreases in Ox V fluorescence also occur at μ Molar dye upon energization of highly purified F_1F_0 ATPase reconstituted into phospholipid vesicles, and also when tetraphenylphosphonium is added to submitochondrial particles. The influence of surface potentials was minimized by screening surface charge with divalent cations. Thus the fluorescence of Ox V can separately monitor surface potentials in response to salts, and diffusion potentials in response to ionophores. Quantitative analysis suggests that upon energization of submitochondrial particles, the fluorescence of Ox V is influenced by local interactions of dye with intramembraneous electrostatic charges, in addition to redistributing and partitioning into the membranes in accordance with the transmembrane voltage. (Supported by AHA)

M-Pos493

NEUROTOXIC GLUTAMATE TREATMENT OF CULTIVATED CEREBELLAR GRANULE CELLS INDUCES THE COLLAPSE OF THE MITOCHONDRIAL MEMBRANE POTENTIAL.
(N.K. Isaev, D.B. Zorov, A.A. Lujin, B.I. Khodorov, I.V. Victorov) Brain Res. Inst. of Acad. Med. Sci. and A.N. Belozersky Inst. Phys.-Chem. Biol. Moscow University, Moscow, Russia. (Spon. by D. Gilbert)

Recently it has been shown that 15-min exposure of cerebellar granule cells to 50 μM glutamate in Mg-free medium induces a sustained decrease in cytosolic pH and fall (about 50%) in the intracellular ATP level (FEBS Letters, 324, 271-273, 1993). In the present work rhodamine 123 was used to monitor the changes in the mitochondrial membrane potential. After 15 min of glutamate treatment the neurons lost their ability to sequester rhodamine 123. Ca^{2+} -ionophore A23187 (20 μM) mimicked the glutamate effect. By contrast 2 mM CoCl_2 prevented the effects of glutamate. The data obtained lead us to suggest that glutamate-induced decrease in ATP level in nerve cells results from Ca^{2+} -induced depolarization of mitochondrial membrane and inability to produce ATP. It seems to be relevant to the phenomenon of an Ca^{2+} -induced nonspecific permeability transitions in mitochondrial membrane which might be one step in the mitochondrial destruction and following process of neuronal death (J. Bioenerg. Biomembr. 24, 119-124, 1992).

M-Pos490

CALCIUM CONTROL OF OXIDATIVE PHOSPHORYLATION IN ISOLATED RAT LIVER MITOCHONDRIA. ((Bart Wise and Alan P. Koretsky)) Dept. of Biological Sciences, Carnegie-Mellon Univ., Pittsburgh, PA 15213. (Sponsored By W. McClure)

Changes in extramitochondrial calcium have been implicated in the control of oxidative phosphorylation, but the mechanism has not been resolved. Using isolated rat liver mitochondria with 1 mM α -ketoglutarate as the substrate, we measured an approximate 30% increase in state 3 respiration when the free calcium concentration was increased from <100 nM to >1.0 μM . However, there was a substantial batch to batch variation with increases ranging from 10% to 48%. With either 10 mM acetoacetate + 2.5 mM β -hydroxybutyrate or with 1.25 mM acetoacetate + 2.5 mM β -hydroxybutyrate as the substrate, no stimulation of respiration was detected with increased calcium. This indicates that the calcium stimulation is substrate dependent and may be due to an increase in mitochondrial redox state, $[\text{NADH}]/[\text{H}^+]/[\text{NAD}^+]$. The mitochondrial redox state is coupled to the $[\beta\text{-hydroxybutyrate}]/[\text{acetoacetate}]$ through the equilibrium maintained by the matrix enzyme β -Hydroxybutyrate dehydrogenase. To characterize the relation between mitochondrial redox state and respiration, the mitochondria were incubated in various ratios of acetoacetate to β -hydroxybutyrate (from 0 to 4) while keeping a constant 2.5 mM β -hydroxybutyrate level. Respiration increased over a 3 fold range as the ratio was made more reduced (lower levels of acetoacetate). The respiration of the mitochondria utilizing acetoacetate and β -hydroxybutyrate at an added ratio of 0.5 was equivalent to the respiration rate of the mitochondria on 1 mM α -ketoglutarate. Future work will include measurement of the $[\beta\text{-hydroxybutyrate}]/[\text{acetoacetate}]$ in order to quantitate the mitochondrial redox state.

M-Pos492

UNCOUPLING OF OXIDATIVE PHOSPHORYLATION BY METALLOTHIONEIN I. ((C.O. Simpkins, Z.H. Liao, C.A. Torrence, C.L. Moore)) Univ. of Maryland Sch. of Med., Dept. of Surgery and Shock Trauma Inst., Baltimore, MD 21205, Morehouse University, Atlanta, GA. 30310. (Spon. by P.M. Sokolove)

Using a Clark-type oxygen electrode we found that electron transfer from succinate to oxygen was enhanced by MT. ADP-initiated oxygen consumption was inhibited by MT. Intracellular concentrations of MT are in the mM range. Below are means \pm S.E. without and with 50 μM MT, in liver mitochondria isolated from 8 different rats.

Succinate (nMole O ₂ /min)		ADP (nMole O ₂ /min)	
No MT	+ MT	No MT	+ MT
27.2 \pm 2.2	47.7 \pm 6.5	82.6 \pm 8.8	57.1 \pm 6.7
$P < 0.05$ for difference between no MT and + MT.			

Experiments were performed at a protein concentration of 0.2mg/ml. Mitochondria were suspended in HEPES 20mM, phosphate (10mM) pH = 7.4, MgCl_2 (5mM), KCl (20mM). ADP was 0.4mM. Succinate was 4mM. Temperature = 25°C. MT is induced by stress. These data support our hypothesis that MT plays a role in the uncoupling of oxidative phosphorylation in stress states.

M-Pos494

EFFECT OF LONG CHAIN OMEGA-3 FATTY ACIDS ON MITOCHONDRIAL BIOENERGETICS. ((W. Stillwell, W.D. Ehringer, T. Crump and L.J. Jenks)) Department of Biology, Indiana University-Purdue University at Indianapolis, Indianapolis, IN 46202

As organisms age their mitochondrial bioenergetic functions deteriorate. Associated with this is an increase in the ratio of saturated/unsaturated membrane fatty acids and a reported decrease in membrane fluidity. Here we report an attempt to reverse the effects of age on bioenergetics by restoring high levels of unsaturated (omega-3) fatty acids to age compromised mitochondria through diet and by fusion with 18:0, 22:6 PC vesicles. Mitochondrial bioenergetic function was followed by respiratory control index (RCI), state 3 respiration, ATP level and phosphate uptake. In addition, lipid composition, phospholipid area/molecule and permeability to protons were also determined. From these experiments we conclude that incorporation of long chain polyunsaturated fatty acids to aged mitochondria not only fail to reverse the deleterious effects of age on mitochondrial function, they may actually further diminish bioenergetic activity.

M-Pos495

A MITOCHONDRIAL EXTRACT PRODUCED BY OSMOTIC SHOCK INDUCES THE RELEASE OF A LIPOSOME-ENCAPSULATED MARKER.
(P.M. Sokolove) Department of Pharmacology & Experimental Therapeutics, University of Maryland Medical School, Baltimore, MD 21201

Liposomes with the composition of the mitochondrial inner membrane [phosphatidylcholine (PC)/phosphatidylethanolamine (PE)/cardiolipin (CL); 4:4:1, mol/mol], containing 10 mM methylumbelliferyl phosphate (MUP), were prepared by extrusion. MUP release was followed via alkaline phosphatase (AP)-mediated cleavage which releases the highly fluorescent methylumbelliferyl anion. A mitochondrial extract (ME) was produced by subjecting mitochondria to osmotic shock in 10 mM Tris-phosphate [Sottocasa *et al.* (1971) *FEBS Lett.* 17: 100]. Exposure of MUP-containing liposomes to ME resulted in an increase in fluorescence, tentatively identified as MUP release, with the following properties: (1) The fluorescence increase required the simultaneous presence of liposomes, ME and AP. (2) The initial rate of MUP release was a saturable function of ME concentration. (3) MUP release was absolutely dependent on inclusion of CL in the liposomes. (4) MUP release was Ca^{2+} independent; it was insensitive to cyclosporin A, spermine, butylated hydroxytoluene, and dithiothreitol. The aim of this investigation was to reconstitute the mitochondrial permeability transition (PT) pore. MUP release was not, however, sensitive to known modulators of the PT. ME may contain the component(s) required for pore formation but lack key regulatory elements. Alternately, MUP release may occur via a different, ME-induced process. [Supported by the American Heart Association - MD Affiliate and the University of Maryland Medical School]

M-Pos497

FAST TWO-DIMENSIONAL DIFFUSION OF H^+ AND WATER ALONG THE MEMBRANE SURFACE: DIFFUSION COEFFICIENT DETERMINATION BY BOUND OPTICAL PROBES, QUASIELASTIC INCOHERENT NEUTRON SCATTERING AND NMR.

((N.A. Dencher, G. Büldt*, Th. Dippel*, J. Fitter*, J. Heberle, R.E. Lechner, D. Oesterhelt*, J. Riesle*, G. Thiedemann*) BENS, Hahn-Meitner Institut, D-14109 Berlin, FRG; *IBI-2, KFA, D-52425 Jülich; †MPI Festkörperf., 7000 Stuttgart; ‡MPI Biochemie, 82152 Martinsried.

Knowledge of the diffusion rate of H^+ and of water along the surface of biological membranes is required for an understanding of energy conversion by the chemiosmotic mechanism. The diffusion coefficient of H^+ along the purple membrane (PM) surface was determined, using optical pH-indicators covalently bound to amino acids of bacteriorhodopsin selectively at position 129 (exposed to the extracellular PM surface) or at the position 36, 38, 161, respectively, of the opposite PM surface. Upon light excitation (8 ns), the H^+ -transfer processes from the active centre of BR to the extracellular side and from there along the membrane-water interphase to the intracellular BR side are kinetically resolved. H^+ ions are diffusing laterally along the membrane surface for long distances (several thousand Å) before equilibrating into the aqueous bulk phase. However, H^+ ions do not move faster than in the aqueous bulk phase. According to quasielastic incoherent neutron scattering and pulsed-field gradient NMR measurements, protons of the hydration water are performing fast anisotropic long-range translational diffusion on the PM surface about 5 times slower than in bulk water, $D_s = 4.4 \cdot 10^{-6} \text{ cm}^2 \text{ s}^{-1}$ at room temperature. The jump distance of about 4 Å for the 2-dimensional long-range diffusion process is larger by a factor 3 than that observed in bulk water.

M-Pos499

M145F MUTANT OF BACTERIORHODOPSIN LOST L-INTERMEDIATE IN PHOTOCYCLE AND SHIFTED DARK-ADAPTATION EQUILIBRIUM

((Kunio Ihara, Naohisa Yamada, Shigeru Itoh*, and Yasuo Mukohata*) Department of Biology, Faculty of Science, Nagoya University, Nagoya 464-01, and *the National Institute of Basic Biology, Okazaki 444, Japan,

Archaerhodopsins¹ are naturally available proton-pumps which are distinct from bacteriorhodopsin (bR). In the dark-adapted state, archaerhodopsin-2 (aR-2) contains retinal isomers at the all-*trans*:13-*cis* ratio of 3:1, whereas bR contains at 1:2. In the retinal pocket the 145th Met on the helix E of bR is the only different amino acid residue which is replaced by Phe in aR-2. The residue should be responsible for the difference in the thermal isomerization equilibrium.

The M145 was thus point-mutated to F. The mutant bR(M145F) actually showed the final ratio of 3:1 in the dark as predicted, although the rate constants differed. In the transient spectra of flash photolysis of bR(M145F), the life time of the K intermediate is too long to show up the L intermediate. The K decay almost corresponds to the rise of the M. The L seems to decay as soon as it formed. bR(M145F) pumps protons in the light as active as bR does.

The 145th amino acid residue of bR interacting with the ionone ring, gives large influences not only on the all-*trans* \rightarrow 13-*cis* (15-*syn*) isomerization process of retinal, but on the photocycle while retinal stays in the form of 13-*cis* (15-*anti*). The authors thank Dr. Richard Needleman of Wayne State University for gracious gift of his *E. coli*/Halobacterium shuttle vector with which bR(M145F) became available. The authors are also indebted to Prof. Gobind H. Khorana and Dr. Mark. P. Krebs of MIT for encouragement in the mutagenesis experiments. 1. Mukohata *et al.*, *Biophys. J.* 53, 376a (1988), *Photochem. Photobiol.* 54, 1039-1045 (1991).

M-Pos496

REVERSIBILITY AND EFFICIENCY IN OSCILLATION INDUCED FREE ENERGY TRANSDUCTION

((Yi-der Chen and Tian Yow Tsong)) NIDDK, NIH, Bethesda, MD 20892 and Hong Kong Univ. of Science and Technology, Kowloon, Hong Kong

It has been shown both experimentally and theoretically that charged transporters that facilitate ligand transport across membranes can absorb energies from an oscillating electric field and use them to pump uncharged ligands actively across the membrane against a concentration gradient (electro-conformational coupling or ECC). Recently, it has been argued that the energy transduction between the oscillating electric field and the ligand transport in an ECC model is reversible and tightly coupled. That is, when the reverse concentration gradient of the ligand is large enough to overwhelm the oscillating potential, energy can efficiently flow from the concentration gradient to the oscillating potential. In this study, the dynamics of an ECC model in the presence of an alternating square electric wave are solved analytically so that the transport flux, the electric energy dissipated, and the energy transduction efficiency of the model can be studied quantitatively. It is found that the reversibility and the degree of coupling of the system depend on the amplitude of the applied oscillating electric field. In general, degree of coupling decreases when the amplitude is decreased and complete coupling occurs only when the amplitude is infinitely large. Also, depending on the rate constants of the model, there may exist a critical amplitude below which the transduction is not reversible. That is, in this case the energy can be transduced from the electrical to the chemical, but not from the chemical to the electric.

M-Pos498

INVERSION OF PROTON TRANSLOCATION IN BACTERIORHODOPSIN MUTANTS D85N, D85T AND D85,96N. ((J. Tittor, D. Oesterhelt and E. Bamberg¹)), MPI für Biochemie D82152 Martinsried and ¹MPI für Biophysik D60596 Frankfurt

Proton translocation activity of bacteriorhodopsin mutants lacking the proton acceptor Asp85 was investigated using the highly sensitive black lipid membrane (BLM) technique. Mutants D85N, D85T and D85, 96 N were constructed and homologously expressed in *Halobacterium salinarum* to yield a membrane fraction with a buoyant density of 1.18 g/cm³, i.e. identical to that of wildtype purple membrane. In all mutants the λ_{max} was red-shifted between 29 and 59 nm compared to wildtype and the pKa of the respective Schiff bases was reduced to 8.3 to 8.9 compared to the value of >13 in wildtype. Therefore a mixture of chromophores absorbing at 410 nm (deprotonated form) and around 600 nm (protonated form) exists at physiological pH. In continuous blue light the deprotonated form generates stationary photocurrents. The currents are enhanced by a factor of up to 50 upon addition of azide in D85N and D85, 96N mutants, whereas D85T shows no azide effect. The direction of these currents is the same as in wildtype. Green light alone is not sufficient to generate stationary currents, but increasing green light intensity in the presence of blue light leads to an inversion of the current. Because all currents are carried by protons, this two photon process proves an inverted proton translocation by BR mutants.

M-Pos500

CHROMOPHORE REORIENTATIONS DURING BACTERIORHODOPSIN PHOTOCYCLE. ((Q. Song, G. Harms, C. Wan, C.K. Johnson)) Dept. of Chemistry, Univ. of Kansas, Lawrence, KS 66045. (Spon. by R.T. Herash)

The anisotropy of bacteriorhodopsin in the purple membranes during the photocycle has been probed by time-resolved linear dichroism and transient absorption measurements in solution. The anisotropies are: the ground state 0.40, K state 0.38, L state 0.34, M state 0.32, O state 0.38, demonstrating chromophore reorientations during the photocycle. Anisotropy decay is observed in the M state from 0.32 to 0.30 in about 0.5 ms, suggesting a chromophore reorientation at this step. The anisotropy of the O state is constant up to 15 ms, indicating a return of the initial chromophore orientation, and a lack of rotational motion of the purple membranes on this time scale. These results provide direct time-resolved evidence for photoinduced chromophore reorientations during the photocycle. At least three steps of reorientational changes take place: a transition from the ground state to the M state; a change in the M state; and a return to the initial orientation upon the formation of the O state. The origins of these photoinduced chromophore reorientations can be either protein reorientations or protein conformational changes during the photocycle. The relevance of these motions to the proton-pumping mechanism is discussed.

M-Pos501

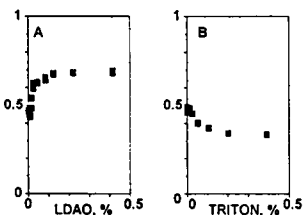
THE J - K TRANSITION IN BACTERIORHODOPSIN, STUDIED BY FEMTOSECOND TIME RESOLVED INFRARED SPECTROSCOPY. ((R. Diller, G. C. Walker, S. Maiti, B. R. Cowen, R. S. Pippenger, R. Bogomolni¹ and R. M. Hochstrasser)) Univ. of Pennsylvania, Philadelphia PA 19104; ¹Univ. of California, Santa Cruz CA 95064. (Spon. by B. Cowen)

The recent years have seen major progress in the application of highly time resolved infrared (IR) spectroscopy to dynamic processes in biological systems (hemoproteins, Bacteriorhodopsin (BR), Reaction Centers). The new Titanium - Sapphire laser technology enables to generate light pulses of few hundred femtoseconds width and a spectral energy density of ca. 10 nJ/nm (8540 nm). This is enough to efficiently pump chromoproteins. We have used this technique together with a continuous wave IR upconversion scheme to extend our picosecond IR studies on BR to the femtosecond regime. We have already observed the very fast bleach of the IR band at 1637 cm⁻¹, the C=NH stretch vibration of BR₅₇₀. Results on the protein response, probed by amide I contributions at around 1660 cm⁻¹ and the dynamics of the J and K intermediate, respectively, as displayed by the absorption features between 1630 and 1580 cm⁻¹ will be presented. This work was supported by NIH, NSF and the Deutsche Forschungsgemeinschaft.

M-Pos503

IS TRITON X-100 A COMPETITIVE INHIBITOR OF ACCEPTOR QUINONE IN REACTION CENTERS OF PURPLE BACTERIA? ((V.P. Shinkarev and C. A. Wraight)) Department of Plant Biology, University of Illinois, Urbana, U.S.A.

The properties of preparations of photosynthetic reaction centers (RCs) of purple bacteria *Rhodospira rubra* depend on type of detergent. To understand differences in the properties of RCs in Triton X-100 and LDAO micelles we investigated the mutual effect of Triton X-100, LDAO and quinone on the time of the P870⁺ dark relaxation in RCs. In the absence of exogenously added quinone (Q_B=0.5 per RC) and starting at low detergent concentration increasing the LDAO concentration leads to increasing the time of the slow component of the P⁺ dark reduction (due to the Q_B⁻ → P⁺ reaction). We suggest that this slowing of recombination time is due to dissolution of RC aggregates that have a faster intermolecular dark relaxation between Q_B⁻ and P870⁺ and switching to the traditional intramolecular electron transfer. In contrast to LDAO, increasing the Triton-X100 concentration, in the absence of added quinone, leads to a decreasing in the time of the slow phase of P870⁺ dark relaxation. We suggested that this effect is due to the competition of Triton X-100 with quinone for "Q_B" binding site, which more than compensates for the effect of dissolving the RC aggregates.



M-Pos505

THE EFFECT OF SR²⁺ SUBSTITUTION ON THE OEC AS STUDIED BY ESEEM ((Michelle Mac, Matthew P. Espe, John L. McCracken and Gerald T. Babcock)) Michigan State University Department of Chemistry, East Lansing, Michigan 48824 (Spon. by C.F. Yocum)

The oxygen evolving complex (OEC) of Photosystem II (PSII) is responsible for catalyzing the photooxidation of water. It consists of a membrane bound complex containing several polypeptides and electron transfer cofactors. Water binding and oxidation are postulated to occur at a site containing 4 Mn atoms. A Ca²⁺ ion, required for normal functioning of the OEC, is associated with the Mn ensemble. The structure of the OEC, as well as the location of the Ca²⁺ with respect to the Mn, has not been completely characterized and is the subject of much dispute. Photooxidation of the OEC results in a paramagnetic state which yields an EPR spectrum consisting of 18-20 lines with an average separation between lines of 85-90 gauss. This "multiline" spectrum can be modified by incubating PSII's with Sr²⁺, which replaces Ca²⁺. These modifications appear as changes in the separation between lines in the EPR spectrum. Pulsed EPR techniques can be used to identify small superhyperfine couplings to the OEC that cannot be observed with continuous wave EPR. Previous ESEEM studies have identified a nitrogen coupling to the OEC which has recently been assigned to the nitrogen moiety of histidine. This interaction was used as a probe to study structural changes of the OEC upon Sr²⁺ substitution. Pulsed EPR studies indicate that these superhyperfine interactions to the nitrogen are unaffected by Sr²⁺ substitution. These results imply that the geometric and/or electronic alterations that cause a change in the EPR spectrum must be small as they do not affect the ligand environment. These results, and their effect on the structure of the OEC, will be discussed.

M-Pos502

MOLECULAR DYNAMICS STUDY OF BACTERIORHODOPSIN AND ARTIFICIAL PIGMENTS. ((W. Humphrey, I. Logunov, K. Schulten and M. Sheves)) Beckman Institute, UIUC, Urbana, IL 61801.

The structure of bacteriorhodopsin, as provided by the so-called Henderson model, is refined using molecular dynamics simulations. The work is based on a previously refined structure which had added the interhelical loops to the Henderson model. The present study applies an all atom description to this structure and constraints to the original Henderson model, albeit with helix D shifted. Sixteen waters are then added to the protein, six in the retinal Schiff base region, four in the retinal-Asp-96 interstitial space and six near the extracellular side. The root mean square deviation between the resulting structure and the Henderson model measures only 1.8 Å. Further simulations of retinal analogues for substitutions at the 2- and 4-positions of retinal and an analogue without a beta-ionone ring agree well with observed spectra. The refined structure is characterized in view of bacteriorhodopsin's function; key features are (1) a retinal Schiff base counterion complex which is formed by a hydrogen bridge network involving six water molecules, Asp-85, Asp-212, Tyr-185, Tyr-57, Arg-82 and Thr-89, and which exhibits Schiff base nitrogen - Asp-85, Asp-212 distances of 6 Å, 4.6 Å; (2) retinal assumes a corkscrew twist as one views retinal along its backbone; (3) a destabilization of the cytoplasmic side of helix G.

M-Pos504

THE VOLUME CONTRACTION ON PHOTOEXCITING BACTERIAL PHOTOSYNTHETIC REACTION CENTERS. ((D. Mauzerall, M. Gunner and J.W. Zhang)) The Rockefeller University, New York, NY 10021 and CCNY, New York, NY 10031.

Reaction centers from *R. sphaeroides* R-26 containing only QA undergo a volume contraction of 20 Å³ mole⁻¹ within <50 ns on photoexcitation as determined by photoacoustics at ~3 C. The sign and rapidity of the change indicate electrostriction as the cause. Using the Drude-Nernst equation, $\Delta V \propto (\partial \epsilon / \partial P) / \epsilon^2$, one concludes that if the interior of the reaction center is a fluid dielectric, it has properties closer to methanol than to benzene. RC's with both QA and QB present also give a negative signal showing the negative signal from RC's having only QA is not caused by the "void" of QB. In the absence of quinones a negative volume change of about 0.4 that with QA is observed. This suggests the triplet state formed under these conditions may have a large ionic character. Replacing QA with various quinones produces volume contractions averaging 0.8 of the natural UQ-10. Again, the exact fit of the quinone does not appear to be critical to the volume contraction, adding support to its cause by electrostriction. Supported by NSF-DMB90-16973 and NIH 5-512RR-A103060.

M-Pos506

STRUCTURAL STUDIES OF PHOTOSYSTEM II ((P.S. Furcinitti, K.M. Marr, M.K. Lyon)) Molecular, Cellular and Developmental Biology, University of Colorado, Boulder, CO 80309 (Spon. by Dr. Michael Seibert) Photosystem II (PS II), a eukaryotic photosynthetic reaction center which converts solar to chemical energy, is also capable of evolving oxygen, making it uniquely important to the biosphere. PS II consists of at least twelve polypeptides and several types of pigments, including chlorophyll. We have been able to form two-dimensional crystals of PS II by detergent treatment. The crystals have been characterized as to polypeptide content, using immunoblot analysis on highly enriched preparations. The crystals consist of at least the D1 and D2 polypeptides, cytochrome b559 and two additional polypeptides with molecular masses of approximately 47 and 43 kDa. Projection maps of samples in both stain and ice have been obtained by low dose electron microscopy. Samples imaged in stain contain information primarily on the portion of the complex protruding from the membrane, while the projection map of frozen, hydrated samples contains information on the total complex. Supported by NIH GM 40735 and NIH Biotechnology Resource Grant RR00592.

M-Pos507

STRUCTURE AND UNPAIRED SPIN DENSITY DISTRIBUTION IN THE STABLE Y_D TYROSINE RADICAL IN PHOTOSYSTEM II ((C.W. Hoganson, M.P. Espe, K. Warncke, J. McCracken and G.T. Babcock)) Dept. of Chemistry, Michigan State Univ., E. Lansing, MI 48824.

The stable redox active tyrosine radical of Photosystem II, Y_D , in purified PSII particles from the cyanobacterium *Synechocystis* 6803, was studied by EPR, ENDOR and ESEEM spectroscopies to determine the unpaired spin density distribution. 2H_2O treatment of the PSII particles reveals a hydrogen bond with $A_1=3.0$ MHz. This value is smaller than the 3.5 MHz seen for Y_D in spinach PSII, suggesting a longer hydrogen bond or lowered spin density on the phenol oxygen. Selective 2H -substitution on the phenol side chain has allowed assignment of the ENDOR features arising from the ring protons meta- to the oxygen. The two largest components of this hyperfine tensor are 7.2 and 4.2 MHz; if the tensor is rhombic the third component is obscured by the much larger matrix peak. 2H -substitution has also shown that the smallest hyperfine tensor component for the protons at the ortho position is ≈ 8 MHz. 2H ESEEM studies reveal that deuteriums in the ortho position have a hyperfine tensor [3.0, 3.9, 1.1] (± 0.2) MHz ([19.5, 23.4, 7.2] MHz for 1H). These values are similar to those reported for the stable tyrosine radical of ribonucleotide reductase (RDPR), showing that the spin density at the ortho- and meta- positions is similar in the two enzymes. Values for Aiso of 1.2 and 3.6 (± 0.2) MHz for both methylene- 2H are obtained from ESEEM studies; the lineshape extents suggests a para- spin density of 0.40 ± 0.04 . EPR spectra from ^{17}O -labeled model tyrosine and in RDPR show ^{17}O couplings of 40 and 43 MHz (spin density -0.28 and 0.30), respectively, and given the comparable ortho- and meta- couplings, suggest comparable values for Y_D . Measurements to determine directly the ^{17}O coupling in Y_D are in progress.

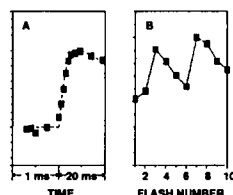
M-Pos509

KINETICS OF THE OXYGEN EVOLUTION STEP *IN SITU* ESTIMATED FROM ITS QUENCHING EFFECT ON FLASH-INDUCED CHLOROPHYLL A FLUORESCENCE ((V. P. Shinkarev, C. Xu, Govindjee and C. A. Wraight)) Department of Plant Biology, University of Illinois, Urbana, IL 61801, USA

Photosystem II (PS II) of oxygenic photosynthetic organisms catalyzes the light-induced splitting of water and the release of oxygen in thylakoid membranes. The major method for measuring flash-induced oxygen evolution in PS II is polarographic, which is limited in time-resolution due

to inclusion of the diffusion time of oxygen molecules to the bulk phase. After an actinic flash, the Chl a fluorescence decays with kinetics that vary with flash number, reflecting events on both the acceptor and donor sides of the reaction center of PS II. Analysis of the flash-induced Chl a fluorescence yield in thylakoids reveals a fluorescence quencher that appears

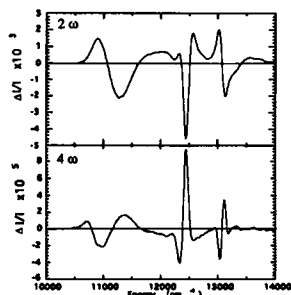
with a lag phase of ≈ 1 ms followed by a rise time of about 2.5 ms (Fig.A). The flash-number dependence of the amplitude of this quencher is characterized by a periodicity of four with maxima after the third and the seventh flashes (Fig.B), suggesting that the quencher is related to the oxygen evolving step of PS II. Thus, measurements of flash-induced oscillations of the kinetics of Chl a fluorescence may provide a new method for measuring the kinetics of oxygen release in PS II *in vivo*.



M-Pos511

HIGHER-ORDER STARK SPECTROSCOPY OF *Rb. sphaeroides* REACTION CENTERS. ((Kaiqin Lao, Laura J. Moore, Huilin Zhou and Steven G. Boxer)) Department of Chemistry, Stanford University, Stanford, CA 94305-5080.

We have developed a technique for observing higher-order Stark spectra in which the amplitude of the Stark signal depends on the fourth or higher even powers of the applied electric field. This technique has been used to study the Q_y bands of *Rb. sphaeroides* R26 and wild-type reaction centers (RCs). The second (2ω) and fourth (4ω) harmonic spectra of R26 RCs are shown in the figure ($T=77K$, $F_{ext}=0.89$ MV/cm, 50% glycerol/buffer, $A=0.08$ at 11363 cm^{-1}). In the fourth harmonic spectrum, the lowest energy band, which is attributed to the special pair (P), has a lineshape which contains significant contributions from the third and fourth derivatives of the absorption spectrum. With this new technique, the higher-order microscopic polarizability tensors can be obtained. Insights into the electronic structure of the special pair obtained from analysis of these higher-order spectra will be discussed.



M-Pos508

LOCATION OF CHLOROPHYLL Z IN PHOTOSYSTEM II ((Dionysios Koulougliotis, Jennifer B. Innes and Gary W. Brudvig)) Dept. of Chemistry, Yale University, New Haven, CT 06511

A chlorophyll, called Chlz, mediates electron transfer between P680⁺ and cytochrome b559 in photosystem II (PSII). The location of Chlz in PSII has been probed by using saturation-recovery EPR to determine the distance between Chlz and the non-heme Fe(II) and by using progressive EPR power saturation measurements to determine the accessibility of Chlz to exogenous Dy^{3+} -EDTA. The EPR signal from Chlz⁺ was induced in dark-adapted, Mn-depleted BBY PSII membranes by illumination at 77 K. Chlz⁺ exhibited non-single exponential spin-lattice relaxation kinetics which were analyzed by using a dipolar model (1,2) to extract the scalar and dipolar spin-lattice relaxation rate constants. The dipolar rate constants showed a $T^{1.6}$ temperature dependence which is identical to that observed for TyrD⁺ in Mn-depleted PSII (1) and P860⁺ in *Rb. sphaeroides* reaction centers (2). This is strong evidence that the non-heme Fe(II) is the relaxation enhancer for all three radicals. By using the known distance between the Fe(II) and P860⁺, we estimate a distance of 40 ± 1 Å between the Fe(II) and Chlz. The effect of Dy^{3+} -EDTA on the progressive EPR power saturation of Chlz⁺ in Mn-depleted (and extrinsic polypeptide depleted) BBY PSII membranes has also been measured. These results show that Chlz⁺ is approximately the same distance from the luminal and stromal surfaces.

Supported by the National Institutes of Health (GM 32715 and GM 36442).

1. D.J. Hirsh, W.F. Beck, J.B. Innes & G.W. Brudvig (1992) *Biochemistry* 31, 532.
2. D.J. Hirsh & G.W. Brudvig (1993) *J. Phys. Chem.*, in press.
3. J.B. Innes & G.W. Brudvig (1989) *Biochemistry* 28, 1116.

M-Pos510

REDOX TITRATION OF CHLOROPLAST THYLAKOID PROTEIN PHOSPHORYLATION: EVIDENCE FOR A SINGLE REDOX-CONTROLLED KINASE AND A REDOX-INDEPENDENT PHOSPHATASE. ((T.P. Silverstein*, Liling Cheng and John F. Allen))

Plant Cell Biol., Lund Univ., S-220 07 Sweden;

*Chem. Dept., Willamette Univ., Salem, OR 97301

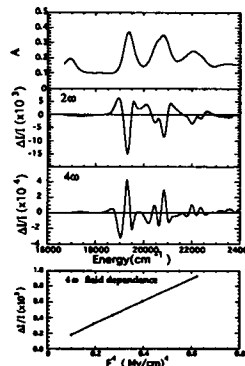
The light-dependent phosphorylation of LHClI is under redox control. We have characterized the redox dependence of both the kinase and phosphatase reactions. We examined LHClI and other prominent thylakoid substrates, including CP43, D1, D2, and others. All phosphoproteins observable by autoradiography and phosphorimaging titrated with roughly the same midpoint potential ($E_m = +40$ mV). While most bands became phosphorylated under reducing conditions ($E_m = +38 \pm 4$ mV, $n = 0.95 \pm 0.06$), two were phosphorylated only under oxidizing conditions ($E_m = +33 \pm 11$ mV; $n = (-) 0.67 \pm 0.09$). One of these "reverse" titrators was a 63 kDa protein, possibly the previously identified [1] 64 kDa redox-controlled kinase. In the presence of the phosphatase inhibitor NaF (10 mM), the redox dependency is essentially unchanged ($E_m = +50 \pm 3$ mV, $n = 1.02 \pm 0.04$). Furthermore, the kinetics of dephosphorylation was independent of redox potential. We conclude that the redox dependency of thylakoid protein phosphorylation derives from a single kinase. Based on the midpoint potentials and n values observed, the controlling redox sensor is either the Q plastosemiquinone in the cytochrome b_6f complex, or else the high potential $cyt\ b_6$ itself.

M-Pos512

HIGHER-ORDER STARK EFFECTS OF CAROTENOIDS IN PHOTOSYNTHETIC ANTENNA COMPLEX. ((Kaiqin Lao, Huilin Zhou, Laura J. Moore and Steven G. Boxer)) Department of Chemistry, Stanford University, Stanford, CA 94305-5080

A new experimental method has been developed in which the Stark spectra of a sample are obtained at different harmonics of the applied AC field. This has

been used to study the carotenoid spheroidene in the B800-850 antenna complex from *Rb. sphaeroides*. The absorption, conventional (2ω) and higher order (4ω) Stark spectra are shown in the figure ($F=0.94$ MV/cm, 50% glycerol/buffer, $T=77K$). Because the spheroidene has an unusually large difference dipole moment in this antenna complex, the 2ω signal is dominated by the second derivative and the 4ω signal by the fourth derivative of the absorption band line shape. We have also observed the field dependence of the 4ω signal, as shown in the bottom panel. This experimental approach has provided a new way to measure the microscopic properties of the molecules, such as the polarizabilities tensors in much greater detail than previously could be obtained.



M-Poe513

ON THE MECHANISM OF MOLECULAR RELAXATIONS IN PHOTOBIOLOGICAL REACTIONS. ((A.P. Demchenko)) Department of Biophysics, Palladin Institute of Biochemistry, Kiev 252030, Ukraine.

Photoinduced charge separation in such structurally unrelated and mechanistically different photosystems, as bacteriorhodopsin and bacterial reaction center, has very important characteristic feature in common: the reaction is divided into a number of steps, and each of them has a duration longer, than the previous one. On each step the probability of the back reactions is very low, which makes the charge separation to be extremely effective. We present a model, in which each step is coupled with the dynamics of protein matrix, with the relaxation rate slower, than the rate of forward, but faster, than the rate of back reaction. Thus the "unrelaxed" charge separation and "relaxed" charge recombination proceed along very different energy profiles. It follows that the back reaction, but not the forward one, may display the features of inhomogeneous (dispersive) kinetics due to slow protein dynamics. This principle may find application in the construction of molecular electronic devices. Quantitative estimates and comparison with the experiment are made.

M-Poe515

ATP-ADP SYSTEM STUDIED BY FOURIER TRANSFORM INFRARED SPECTROSCOPY. (M.T. Fornoni, D. Origi, A.M. Villa, and S.M. Doglia). Physics Dept. of the University and Consorzio Bioricerche, Milano, Italy.

ATP hydrolysis is a central biochemical process occurring in living cells in all phosphates transferring reactions. We propose a new method to evaluate the ATP-ADP concentrations by Fourier Transform Infrared (FT-IR) Spectroscopy, a non destructive technique that can be applied to the study of ATP-ADP system in water solution and also in intact living cells. The method is based on the difference in the IR absorption spectra of ATP and ADP, that for concentrations below 100 mM, also in the spectral region 1300-800 cm^{-1} outside the strong absorption of water, can be appreciated only after water subtraction. An FT-IR interferometer (Digilab FTS-40A) in attenuated total reflection (ATR), equipped with an horizontal ZnSe cell, has been employed in order to perform a controlled and reproducible water subtraction. The FT-IR spectra of ATP and ADP solutions, at millimolar concentrations, display then a difference particularly evident in the absorption region of the antisymmetric stretching vibration of the P-O-P group (850-970 cm^{-1}), where the ATP band at 918 cm^{-1} is well separated from the ADP at 937 cm^{-1} . This difference in the spectral response allows to evaluate the ATP-ADP concentrations by FT-IR. As an example, results obtained in attenuated total reflection on the ATP hydrolysis induced by the hexokinase reaction will be presented and compared with results obtained by the optical absorption method based on an acid base indicator (cresol red). Possible applications in living cells will be discussed.

MEMBRANE AND TRANSPORT ATPases

M-Poe516

MEASURING ELECTRONEUTRAL ION FLUX FROM ISOLATED EPITHELIAL CELLS WITH A VIBRATING ION-SELECTIVE ELECTRODE. ((J.L.M. Morgan, A. Shipley and J.R. Demarest)) Dept. Biol. Sci., University of Arkansas, Fayetteville, AR 72701 and "Nat. Vibr. Probe Fac., MBL, Woods Hole, MA 02543.

Epithelial cells are frequently studied in isolation where it is difficult to monitor their normal function, i.e. transcellular transport. Patch clamp studies of membranes of isolated cells can be used to investigate conductive ion channels, but not slower passive exchange or active transport mechanisms. Vibrating ion-selective electrodes can be used to measure extracellular ion gradients from which flux generated by such mechanisms can be determined. We have used vibrating (≤ 0.5 Hz) H^+ -selective liquid ion-exchange electrodes to measure the H^+ flux generated by the electroneutral H^+/K^+ -ATPase of the apical membrane of single isolated *Necturus* gastric oxyntic cells. Histamine (10^{-4} M) and cAMP (10^{-3} M) increased metabolically dependent apical, but not basolateral, H^+ flux by ~ 60 and $>200\%$. Stimulated H^+ secretion reached a steady level at 30-40 minutes and was inhibited to resting levels by SCH28080 (10^{-4} M), a specific H^+/K^+ -ATPase blocker. Proton flux decreased as a function of the distance from the apical surface of secreting cells as expected for simple and facilitated diffusion of protons from the cell surface due to the inclusion of pH buffers (1 mM HEPES and 5 mM HCO_3^-) in the bathing solution. The influence of current flow, due to electrogenic Cl^- secretion by the cells, on the H^+ flux measurements was assessed using Ba^{2+} (0.5×10^{-4} M). Membrane potential of isolated cells was depolarized from -53 ± 3 to -26 ± 5 mV by Ba^{2+} , but Ba^{2+} did not significantly effect the measured H^+ flux. Vibrating ion-selective electrodes should prove useful for functional studies of other electrically silent transporters in single isolated cells. (Supported by NIH BRSG07RR071011, DK38664, and MBL Summer Fellowship)

M-Poe514

EXPERIMENTAL AND THEORETICAL INVESTIGATIONS OF SELF-ORGANIZATION PHENOMENON IN OPEN BIOMOLECULAR SYSTEMS OF CHARGE TRANSPORT. ((V.N. Kharkyanen)) Scientific Research Center "Vidhuk", Volodymyrska St., 61-b, Kiev 252033, Ukraine (Spon. by A.P. Demchenko)

The results of theoretical and experimental study of new phenomenon, the self-organization in the open biomolecular systems of charge transport, are presented. Due to the strong influence of the flux of the charged particles on the protein structure in the systems of electron, proton and ion transfer, the flux interacts with the slow protein modes, which generates new stationary states. These new stationary states of macromolecules differ fundamentally from the equilibrium ones and appear only after the the stationary charge flux exceeds its critical value. The characteristic features of this phenomenon are bistability, oscillatory behavior and dynamic chaos, which determine the functional efficiency. The observation of this phenomenon and its influence on some physical properties of reaction centers of purple bacteria are discussed. The most interesting of them is the non-linear effect of illumination after the charge current reaches some critical value.

M-Poe517

NA,K-ATPASE CATALYTIC ISOFORMS HAVE DISTINCT INTERACTIONS WITH K^+ . ((S.E. Daly¹, J.S. Munzer¹, E.A. Jewell², J.B. Lingrel² and R. Blostein¹)) ¹McGill Univ. Montreal, Canada and ²Univ. of Cincinnati, Cincinnati, OH.

The expression in HeLa cells of the three isoforms of the catalytic α subunit of the Na,K-ATPase has provided a useful means of examining the behavior of the individual isoforms (Jewell & Lingrel, J Biol Chem 266: 16925, 1991; ref. 1). One region of marked diversity among the otherwise closely homologous isoforms is the lysine-rich NH_2 -terminus. Interestingly, tryptic removal of this region from the kidney ($\alpha 1$) enzyme results in a modified enzyme (α_{mod}) with a lower K_{ATP} and markedly less inhibition by K^+ at low [ATP], indicating a role of the NH_2 -terminus in the K^+ deocclusion pathway of the reaction (Wierzbicki & Blostein, Proc Nat Acad Sci 90: 70, 1993; ref. 2). Accordingly, we have examined further the ligand interactions using the individual isoform-transfected HeLa cells, in particular the effects of K^+ at low [ATP] (Na^+ -ATPase), and the extracellular K^+ (K_{ext}) and cytoplasmic Na^+ (Na_{cyt}) activation of Na/K pump activity, with the following results: (i) $\alpha 2$ resembles α_{mod} with respect to K^+ effects on Na^+ -ATPase at low [ATP] and lower K_{ATP} compared to $\alpha 1$. (ii) $\alpha 3$ has $\alpha 1$ -like K^+ -inhibition of Na^+ -ATPase, but like $\alpha 2$, a lower K_{ATP} compared to $\alpha 1$. (iii) $\alpha 3$ has a higher apparent affinity for K_{ext} compared to $\alpha 1$ or $\alpha 2$ (lower K_{K} for K^+ -activation of Na,K-ATPase measured at high [ATP] (ref. 1) and lower $K_{\text{K}}(\text{ext})$ for Na/K exchange in intact cells). As well, the affinity of $\alpha 3$ for Na_{cyt} is ≈ 5 fold lower than that of $\alpha 1$ or $\alpha 2$. Taken together, these observations are consistent with the conclusion that the basic difference between $\alpha 2$ and $\alpha 1$ is the lower K_{ATP} of $\alpha 2$ such that K^+ deocclusion from $\alpha 2$ [$\text{E}_2(\text{K}) \xrightarrow{\text{ATP}} \text{E}_2\text{K} \rightarrow \text{E}_1\text{K}$] is less rate-limiting at low ATP (c.f. ref. 2); $\alpha 3$, on the other hand, probably differs from both $\alpha 1$ and $\alpha 2$ in its 'intrinsic' $\text{K}_{\text{K}}(\text{ext})$ for dephosphorylation [$\text{E}_2\text{P} + \text{K}_{\text{ext}} \rightarrow \text{E}_2(\text{K}) + \text{P}_i$]. The $\alpha 1$ -like K^+ -inhibition of $\alpha 3$, despite its lower K_{ATP} compared to $\alpha 1$, probably reflects inhibitory K^+ interactions (competition?) at cytoplasmic Na^+ sites which, in this isoform, have a lower affinity for Na_{cyt} [$\text{E}_1 + \text{K}^+ \rightarrow \text{E}_1\text{K} \rightarrow \text{E}_2(\text{K})$]. Supported by MRC (Canada) and NIH.

M-Pos518

THE MECHANISM OF Na^+ INTERACTION WITH FLUORESCIN 5'-ISOTHIOCYANATE-MODIFIED DNA, K-ATPASE. (I.N. Smirnova, S.H. Lin and L.D. Faller) CURE, UCLA Dept. Med. & VAMC WLA Wadsworth Div., Los Angeles, CA 90073.

We have previously shown that 2 K^+ ions must bind to cause the conformational change in Na,K-ATPase reported by FITC modification (*JBC* 268, 16120, 1993). Here we report that at least 2 Na^+ ions bind to shift the equilibrium back from the E_2 to the E_1 conformation. Reversal of the fluorescence quench caused by K^+ has been studied by mixing FITC-labeled enzyme preincubated in K^+ with Na^+ . There is an inverse relationship between the empirical first order rate constant and $[\text{Na}^+]_0$. The magnitude of the fluorescence change depends sigmoidally on $[\text{Na}^+]_0$. The simplest model that can explain these results assumes competitive binding of 2 K^+ and 2 Na^+ ions to identical and independent sites on E_1 . The Na^+ dissociation constant (K_{Na}) estimated from the sigmoidal dependence of fluorescence change on $[\text{Na}^+]_0$ is 0.32 mM, in good agreement with values estimated from direct measurements of Na^+ binding. The predicted half-maximum $[\text{Na}^+]_0$ in equilibrium titrations depends on $[\text{K}^+]_0$ and the forward (k_f) and reverse (k_r) rate constants because of coupling to the conformational change and is larger than K_{Na} . The predicted half-maximum $[\text{Na}^+]_0$ for reversal of the quench caused by 30 mM K^+ at 15 °C is 66 mM compared with an observed value of 74 mM. The other estimates used in the calculation are $K_R = 5$ mM, $k_f = 142 \text{ s}^{-1}$, and $k_r = 0.12 \text{ s}^{-1}$. Supported by NSF, NIH and VA.

M-Pos520

TRANSIENT CURRENTS MEDIATED BY THE Na^+/K^+ PUMP IN INTERNALLY-PERFUSED *XENOPUS* OOCYTES. (M. Holmgren and R. F. Rakowski) Univ. Health Sci./Chicago Med. Sch., N. Chicago, IL 60064.

Pre-steady-state transient currents have been investigated in the vegetal pole of *Xenopus* oocytes using the open-oocyte vaseline-gap technique. Voltage pulses 40 ms in duration were made from a holding potential of -40 mV to command potentials over the range -160 to +60 mV in increments of 20 mV. Current records in the presence of dihydroouabain (DHO) or absence of external Na^+ (Na_0) were subtracted from current records obtained under Na^+/Na^+ exchange conditions, i.e. internally perfused with 50 mM Na^+ , 5 mM ATP, and 5 mM ADP (K^+ -free) and externally superfused with 100 mM Na^+ , K^+ -free solution. Transient currents were dependent on intracellular Na^+ and nucleotides, and diminished by activation of forward pumping; they were also reduced by $10 \mu\text{g ml}^{-1}$ of external oligomycin B. The voltage dependence of the transient currents was analyzed using a pseudo two-state model in which only the rate coefficient for Na_0 -binding/reocclusion is voltage dependent. The apparent valences of the charge moved during the on and off of the pulse were 0.96 ± 0.05 and 0.95 ± 0.05 for Na_0 -sensitive, and 1.10 ± 0.07 and 0.85 ± 0.06 for DHO-sensitive transient currents. The total amount of charge moved and the mid-point voltage of the charge distribution (V_q) were $230 \pm 15 \text{ pC}$ and $-56.2 \pm 5.1 \text{ mV}$, and $268 \pm 34 \text{ pC}$ and $-67.0 \pm 7.6 \text{ mV}$ for Na_0 - and DHO-sensitive transient currents, respectively. The apparent valence and the voltage at which the forward and backward rates are equal (V_k) obtained from the current relaxation rates were 0.80 ± 0.05 and $-129.3 \pm 10.0 \text{ mV}$, and 0.86 ± 0.10 and $-135.1 \pm 9.0 \text{ mV}$ for the Na_0 - and DHO-sensitive pre-steady state currents, respectively. The discrepancy between V_q and V_k is not compatible with a simple two-state model for charge movement. Supported by NIH Grant NS-22979.

M-Pos522

CONFORMATION AFFECTS PHOSPHORYLATION OF Na,K-ATPase BY KINASES. (M.S. Feschenko and K.J. Sweadner) Neurosurgical Research, Massachusetts General Hospital, Boston, MA 02114 USA.

Phosphorylation catalyzed by protein kinases can be one of the mechanisms for regulation of Na,K-ATPase activity. The link between physiological effects caused by protein kinase stimulation and direct phosphorylation of the ATPase molecule is still to be found. We observed phosphorylation of the α_1 -subunit of rat kidney pump by cAMP dependent protein kinase (PKA) and protein kinase C (PKC) *in vitro*. In both cases phosphorylation was dependent on the ATPase conformation. Conditions favorable for E_2 -conformation, in particular the presence of ouabain, result in a dramatic increase in phosphorylation by PKC. In contrast, PKA-induced phosphorylation was significantly decreased by ouabain. The data suggest that phosphorylation by PKC and PKA occurs at different sites of the molecule. The preferential exposure of target sites in different conformations suggests that susceptibility to kinase-mediated regulation may depend on the physiological state: i.e. on whether the pump is active or resting. This predicts complex responses to kinase activation *in vivo*.

M-Pos519

COMPARISON OF THE Na/K PUMP CLONED FROM *XENOPUS* KIDNEY WITH THE ENDOGENOUS Na/K PUMP IN *XENOPUS* OOCYTES. (A. Sagar and R. F. Rakowski) Univ. of Health Sciences/Chicago Medical School, N. Chicago, IL 60064

In order to determine if α and β subunit clones of the Na,K-ATPase isolated from *Xenopus* kidney are phenotypically identical to the endogenous Na,K-ATPase found in *Xenopus* oocytes, the activation of Na/K pump current by extracellular $[\text{K}]$ in Na-free solutions was studied in *Xenopus* oocytes using a two microelectrode voltage clamp. *Xenopus* kidney (α) and β cDNA were obtained by *in-vitro* transcription from the cloned cDNA. Oocytes were injected with 5-10 ng of α_{XK} and 1 ng of β_{XK} in 50 nl of RNase-free water. Control oocytes were injected with 50 nl of RNase-free water. All solutions contain (in mM) 20 tetraethylammonium sulfate, 5 BaCl₂, 5 Tris/Hepes, 0.3 nitric Acid, and 120 tetramethylammonium (TMA) sulfate. $[\text{K}]$ was varied between 10 and 0.15 mM (TMA substitution for K). I-V relationships were measured in Na-loaded oocytes over the range -160 to 0 mV from a holding potential of -40 mV. Pump current (I_p) was measured by subtraction of the current in K-free solution from that at various $[\text{K}]$. In Na-free solutions I_p can be described by the equation: $I_p = E/(1 + (a/c))$, where E is proportional to the pump site density, a is the pseudo-two-state forward rate constant, and c is the forward rate coefficient for K translocation given by $c = c(0) [K]^{1/\lambda_K} \exp(-\lambda_K \lambda_K FV/RT)$. $c(0)$ is an intrinsic voltage independent rate constant, λ_K is the Hill coefficient, and λ_K is the mean fractional depth of the external access channel for K. The above equations were fitted to I-V data from 4 control oocytes and 4 oocytes injected with $(\alpha + \beta)_{\text{XK}}$ cDNA. Control measurements of the endogenous pump yielded $E = 0.375 \pm 0.003 \mu\text{A cm}^{-2}$, $c(0)/a = 1.4 \pm 0.08 \text{ mM}^{-1} \lambda_K$, $\lambda_K = 1.13 \pm 0.04$, and $\lambda_K = 0.333 \pm 0.012$. The endogenous I_p can be subtracted from the total current measured in oocytes injected with $(\alpha + \beta)_{\text{XK}}$ cDNA. This gave: $E = 1.19 \pm 0.03 \mu\text{A cm}^{-2}$, $c(0)/a = 0.94 \pm 0.07 \text{ mM}^{-1} \lambda_K$, $\lambda_K = 0.78 \pm 0.05$, and $\lambda_K = 0.339 \pm 0.023$. The close agreement of the values of λ_K allows the conclusion that the access channel depth of the cloned α_{XK} subunit is the same as that of the endogenous Na,K pump. The differences in the measured values of $c(0)/a$ and λ_K may arise from differences in the cloned β_{XK} subunit (β_1 isoform) and the endogenous β_3 isoform. Supported by NIH Grant NS-22979.

M-Pos521

Na/K PUMP IS STIMULATED BY ISOPROTERENOL IN RAT VENTRICULAR MYOCYTES. ((J. R. Stimers and S. Liu)) Department of Pharmacology & Toxicology and Division of Cardiology, University of Arkansas for Medical Sciences, Little Rock, AR.

β -Adrenergic stimulation of the Na/K pump in adult rat ventricular cardiac myocytes was studied using the whole cell patch clamp technique. Myocytes were voltage clamped at -40 mV and perfused at 37 °C with Ca-free HEPES buffered solution containing (in mM) 150 Na, 5.4 K, 1 Ba and 0.1 Cd (Ca-free) to minimize membrane currents other than the Na/K pump current (I_p). Patch electrodes of 2-3 M Ω resistance were filled with mM: 50 Na, 100 Cs, 30 Cl, 130 Aspartate, 10 HEPES, 1 EGTA, 5 ATP and 0.5 GTP. I_p was measured by subtracting the currents recorded in response to 300 ms pulses between -130 and +50 mV elicited in Ca-free solution with 1 mM ouabain from similar currents recorded without ouabain. Results of these measurements gave results similar to those previously reported by ourselves and others. Under these conditions I_p was about 1 pA/pF at 0 mV. Application of 10 μM isoproterenol caused the holding current to move more positive. Repeating the procedure described above to measure I_p , we found that in the presence of isoproterenol I_p was increased at all potentials and was 1.7 pA/pF at 0 mV. These results suggest that β -adrenergic agonists can stimulate the Na/K pump under these conditions. Further tests are needed to determine the mechanism of this coupling. (Supported by NIH grant HL44660)

M-Pos523

ELECTROPHYSIOLOGICAL AND BIOCHEMICAL EFFECTS OF ALTERING THE RATIO OF Na/K PUMP α SUBUNITS. ((T.A. Kinard and J.R. Stimers)) Department of Pharmacology and Toxicology, Univ. of Arkansas for Medical Sciences, Little Rock, AR 72205.

The ratio of the Na/K pump α subunits was altered by making rats hyperthyroid by a daily subcutaneous injection of triiodothyronine (T3, 1.0 $\mu\text{g/g}$ for 7 d) which has been shown in previous biochemical studies to reduce the ratio of $\alpha_1:\alpha_2$ from 12:1 to 1:1 in which the abundance of α_2 increases 10 fold with little effect on α_1 . Using the whole-cell patch-clamp technique the electrophysiological effects were determined by measuring Na/K pump current (I_p) in rat ventricular myocytes voltage clamped at -40 mV and maintained at 37°C. Solutions containing 2 mM Ba, 0.1 mM Cd and 0 Ca were used to block Ca and K currents to improve the isolation of I_p . The electrophysiological studies we conducted (ouabain affinity, K_o dependence of I_p , and K_o dependence of voltage dependence of I_p) showed an apparent increase in the abundance of functional α_2 subunits, but only about 1.6 fold in maximum I_p . Due to the discrepancy of the biochemical and electrophysiological data using hyperthyroid rats we measured the apparent affinity (K_o) of ouabain binding to the α_2 subunit of the Na/K pump and the concentration of ouabain binding sites (B_{max}) of the α_2 subunit using [³H]ouabain binding. Altering the ratio $\alpha_1:\alpha_2$ subunits of the Na/K pump did not change K_o , however B_{max} did increase 1.7 fold due to hyperthyroidism in agreement with our electrophysiological data. (Supported by UAMS and NIH Grant HL44660).

M-Poe524

3D MOLECULAR ARCHITECTURE OF CALCIUM REGULATION IN THE GUINEA PIG BLADDER SMOOTH MUSCLE CELL. E.D.W. Moore, M.F. Wendt-Gallitelli*, G. Isenberg* and F.S. Fay. Dept. of Molecular Med. U. of Mass. Med. School, *Dept. of Physiol., U. of Tübingen, and *Dept. of Physiol., U. of Cologne.

We have examined the distribution of the $\text{Na}^+/\text{Ca}^{2+}$ exchanger, the Na^+/K^+ pump, caveolin, calsequestrin and vinculin in single smooth muscle cells isolated from the bladder of the guinea pig. Following enzymatic dissociation, 100-150 μl of cell suspension was layered onto poly-L-lysine coated cover slips for two hours prior to fixation with 2% paraformaldehyde. Indirect immunofluorescence techniques were used to visualize the indicated proteins. To examine the distribution of these proteins we obtained a series of 2D images through focus with a Nikon Diaphot 300 wide-field microscope, to which we applied a deconvolution algorithm, based on regularization theory, to remove the out of focus fluorescence. The resulting high resolution 3D images indicate that each of these proteins was located on or near the cell membrane in a highly organized fashion. All of these proteins were organized into strands running roughly parallel to the long axis of the cell. Individual strands often bifurcated and were roughly 1 μm apart. Data detailing the distribution of these proteins relative to each other, and to intracellular organelles will be presented. Supported by a Grant-in-Aid from the AHA to EDWM, NATO CRG930985 to MFWG and GI, and HL14523 to FSF.

M-Poe526

^{18}O MEDIUM EXCHANGE STUDY OF THE INTERACTION OF $\text{Na}_2\text{K-ATPASE}$ WITH PHOSPHATE. (V.N. Kasho and M. Stengelin) CURE, UCLA Dept. Med. & VAMC WLA Wadsworth Div., Los Angeles, CA 90073. (Spon. by L.D. Faller)

^{18}O medium exchange catalyzed by $\text{Na}_2\text{K-ATPase}$ from pig kidney has been reinvestigated by gas chromatography mass spectrometry (Stempel and Boyer, 1986, Methods in Enzymology 126, 618). The advantage of GCMS compared to older methods is that the distribution of inorganic phosphate into the five species with from zero to four ^{18}O atoms can be detected with less than 2% error. This makes it possible to characterize ^{18}O exchange not only by an exchange rate, but also by a distribution coefficient P_e (Hackney, 1980, JBC 255, 5320). Under standard conditions ($T=25^\circ\text{C}$, pH 7.4, 10 mM potassium, 200 mM ionic strength) the P_e was 0.24 ± 0.04 ($n=58$). P_e is independent of the magnesium or phosphate concentration, however, it showed as reported earlier (Dahms and Miara, 1983, Curr. Top. Membr. Transp. 19, 371) a strong pH dependence ($P_e=0.55$ at pH 5.5, $P_e=0.03$ at pH 8.5). The exchange rate under optimal conditions was 24 units ($\mu\text{atoms per min.}$) per mg ($T=25^\circ\text{C}$) for a preparation with a specific activity of 17 units per mg ($T=37^\circ\text{C}$). The substrate for medium exchange is free phosphate, not magnesium phosphate. Half-saturating free magnesium concentration at a free phosphate concentration of 2 mM is 1 mM, and half-saturating free phosphate concentration is 1.3 mM at a free magnesium concentration of 5 mM. Supported by NSF, NIH and VA.

M-Poe528

REDUCED Na_2PUMP ACTIVITY PRODUCED BY INHIBITION OF PROTEIN GLYCOSYLATION. (Carlos H. Pedemonte) Department of Pharmacology, University of Houston, Houston, Texas 77204-5515.

The short circuit current (SCC), a measure of the sodium translocation across epithelia, was reduced in cells treated with Tunicamycin (TM), an inhibitor of the process of protein glycosylation. A6 cells, grown on permeable membranes, were treated with TM. After 24 h, the SCC across the A6 monolayer was nearly zero. Amphotericin B was added to the apical surface of the cell monolayer. This treatment permeabilized the A6 apical membrane to sodium, and allowed us to measure the Na-pump at saturating sodium concentration. In this condition, the SCC was a direct measurement of the maximum Na-pump activity. The Amphotericin B treatment released most of the SCC inhibition, but the 25% reduction of the SCC still remaining was evidence of a reduced Na-pump activity. Treatment of A6 cells with TM for 72 h, resulted in a 75% inhibition of the Na-pump activity. Treatment of A6 cells with Amiloride to inhibit the apical sodium channel did not produce an inhibition of the Na-pump similar to the one observed after TM treatment. Therefore, the inhibition of the Na-pump activity by TM was not secondary to the inactivation of the sodium channel. The number of Na-pump molecules at the cell membrane was determined by ouabain binding. After 72 h. of TM treatment, a reduction of both ouabain binding and $\text{Na}_2\text{K-ATPase}$ activity was observed. The lower $\text{Na}_2\text{K-ATPase}$ activity and reduced number of Na-pump molecules were consistent with the reduced SCC produced by TM and measured in the presence of Amphotericin B. These results suggest that inhibition of the protein glycosylation interferes with the synthesis or processing of the Na-pump.

M-Poe525

VOLTAGE DEPENDENCE OF THE TWO Na-K PUMPS WHICH COEXIST IN GUINEA PIG VENTRICULAR HEART CELLS. (J. Shi, R.T. Mathias, I.S. Cohen, J. Gao and G.J. Baldo) Dept. of Physiology & Biophysics, HSC, SUNY at Stony Brook, NY 11794-8661. (Spon. by G.J. Baldo)

The access channel model (Gadsby, et al., 1993, Science 260:100) is used to describe our data. At normal $[\text{Na}]_o$, hyperpolarization decreased pump current by increasing $[\text{Na}]$ in the voltage well, thus increasing the pump back flux. Two counter effects contribute to the voltage dependence of K^+ activation. First, depolarization or removal of $[\text{Na}]_o$ shifts occupancy from the Na^+ -release states to the K^+ -binding states, thus making more pumps available for K^+ binding. We will refer to this as the kinetic effect. Second, depolarization decreases $[\text{K}]$ near the K^+ binding site, which is also in a voltage well, resulting in less K^+ binding. When external Na^+ is removed, the kinetic voltage dependence of K^+ activation is removed, thus allowing us to observe only the voltage well effect. Conversely, when $[\text{K}]_o$ is saturating, we measure the voltage dependence of Na^+ release only. Our data were fit with the Albers-Post cycle assuming three independent sites for Na^+ . For the low affinity type pumps each Na^+ traveled through 30% of the membrane electric field in the voltage well whereas the distance was 42% for the high affinity pumps. Data were adequately fit by assuming that K^+ travels the same depth into voltage wells. With these parameters, we accurately predict the over-all voltage dependence of the normal Na/K pump current when $[\text{Na}]_o=140\text{mM}$ and $[\text{K}]_o=4.6\text{mM}$. Given the distances traveled by Na^+ and K^+ within the membrane's electric field, other steps in the pump cycle must be voltage dependent, but these steps are normally at saturating rates so their voltage dependence is not observed. Supported by NIH grants HL20558 & HL28958 and the American Heart Association.

M-Poe527

DIETARY CHOLESTEROL AND Na^+/K^+ PUMP FUNCTION IN VENTRICULAR MYOCYTES.

(David F. Gray, Livia C. Hool & Helge H. Rasmussen) Department of Cardiology, Royal North Shore Hospital, Sydney, Australia.

Both stimulatory and inhibitory effects of cholesterol on isolated $\text{Na}^+/\text{K}^+/\text{ATPase}$ have been reported. Since serum cholesterol influences cell membrane cholesterol content, we speculated that changes in serum cholesterol may alter Na^+/K^+ pump activity in intact cells. We measured Na^+/K^+ pump currents (I_p) in isolated ventricular cells from control rabbits (serum cholesterol 0.90 ± 0.12 mmol/l, mean \pm SE), and from rabbits fed a high cholesterol diet for one week (serum cholesterol 6.92 ± 1.15 mmol/l). Myocytes were voltage clamped at -40 mV with wide-tipped patch pipettes (4-5 μm , ~1.0 M Ω resistance). They were internally perfused with a pipette filling solution containing a near-physiological Na^+ concentration of 10 mM. I_p was identified as the shift in holding current induced by 50 μM ouabain. I_p , normalised for membrane capacitance (C_m) was 0.33 ± 0.02 pA/pF ($N=11$) in myocytes from control rabbits, and 0.51 ± 0.03 pA/pF ($N=40$) in myocytes from cholesterol fed rabbits ($P<0.005$). C_m of cells from control and cholesterol fed rabbits were not significantly different (141 ± 16 vs 128 ± 6 pF, $P>0.5$). I_p of myocytes from control and cholesterol fed rabbits were similar when pipette filling solutions were Na^+ free (0.06 ± 0.02 , $N=7$ vs 0.08 ± 0.02 pA/pF, $N=7$) indicating that the cholesterol effect on I_p when pipette Na^+ was 10 mM was not due to enhanced passive Na^+ influx. We conclude that diet-induced changes in serum cholesterol can alter electrogenic Na^+/K^+ pumping in cardiac myocytes.

M-Poe529

PARTIAL PURIFICATION OF A PS-STIMULATED, VANADATE-SENSITIVE ATPASE. (J. V. Lyles and D. L. Daleke) Department of Chemistry, Indiana University, Bloomington, IN 47405.

Phospholipids in biological membranes are asymmetrically distributed across the membrane bilayer: choline-containing phospholipids reside preferentially in the outer monolayer while amine-containing phospholipids are found primarily in the inner monolayer. This membrane asymmetry is maintained in part by an inwardly-directed ATP-dependent aminophospholipid transporter that is selective for phosphatidylserine (PS) and inhibited by vanadate. An 83-fold purification of a candidate transporter, a PS-stimulated, vanadate-sensitive ATPase, has recently been achieved from human erythrocytes using anion exchange and gel filtration chromatography. The partially purified ATPase exhibits a specific activity of 299 nmol/min/mg and contains five major proteins (165, 83, 47, 42, and 32 kDa). Candidate transporters have been identified by photoaffinity labeling with azido-ATP. In previous reports a 120 kDa protein was identified as the candidate transporter. Using the purification methods described above, however, PS-stimulated, vanadate-sensitive ATPase activity has been separated from the 120 kDa protein. Furthermore, the 120 kDa protein has been identified as ATP citrate lyase based on partial sequence analysis, enzymatic activity, and immunoreactivity with anti-ATP citrate lyase antibodies. Positive identification of the aminophospholipid transporter awaits reconstitution of the candidate ATPase and demonstration of flippase activity.

M-Pos530

EFFECTS OF SULFHYDRYL REAGENTS ON THE H⁺-ATPase OF *Kluyveromyces lactis*. GUERRA, G., URIBE, S. AND PARDO, J.P. Departamento de Microbiología. Instituto de Fisiología Celular. Universidad Nacional Autónoma de México. Apartado 70-242. 04510 México D.F. (Spon. by A. Peña).

The H⁺-ATPase from *K.lactis* is constituted by a 100 Kda subunit which alternates between states E₁ and E₂. Most aminoacid residues playing a direct role in the reaction cycle of H⁺-ATPase are unknown. SH-reagents methylmetane thiosulfonate (MTS), N-ethylmaleimide (NEM), iodoacetamide and IAEDANS were used to test the reactivity of the cysteine residues of the plasma membrane H⁺-ATPase from *K.lactis*. The modification of cysteine residues with bulky sulfhydryl reagents (NEM and IAEDANS) rapidly inhibited the ATPase, with a pseudo-first order kinetics. In both cases, the H⁺-ATPase was partially protected by Mg-ADP. In contrast, iodoacetamide caused a slight inhibition. Modification of the SH groups on the ATPase by MMTS resulted in an enzyme with full activity. Furthermore, the MMTS-enzyme is resistant to the nucleophilic attack by NEM. These results suggest that there are cysteine residues near the active site which may not be essential for enzymatic activity. MMTS did not protect the enzyme against IAEDANS inhibition. The inactivation reaction was independent of the pH suggesting that IAEDANS reacted with a methionine residue inactivating the enzyme.

M-Pos532

Mitochondrial ATPase Dependent Iron Transport from Proteoliposomes. ((C-Y Li, J.A. Watkins, and J. Glass.)) Department of Medicine, LSU Medical Center, Shreveport LA. 71130.

The rabbit reticulocyte H⁺-ATPase reconstituted into liposomes demonstrates Fe transporter activity with Fe(II) transport greater than Fe(III). The following studies were performed to determine if Fe transport was specific for the reticulocyte H⁺-ATPase. When the bovine heart mitochondrial ATPase was reconstituted into soybean phospholipid liposomes, the proteoliposomes showed Fe transport activity dependent on the presence of the mitochondrial ATPase. Fe transport from the proteoliposomes at 2.5 hrs was 51 ± 0.8% for ⁵⁹Fe³⁺ and 44 ± 1.8% for ⁵⁹Fe²⁺ of trapped Fe, corresponding to 0.013 μmole of Fe³⁺ and 0.011 μmole of Fe²⁺ transported per mg ATPase. Passive transport of iron from the liposomes at 2.5 hours was 5.6 ± 2.0% for Fe³⁺ and 4.5 ± 1.0% for Fe²⁺. Transport was sensitive to inhibitors of the mitochondrial H⁺-ATPase. The initial transport rate decreased to 66.3 ± 5.5% at 50 μM DCCD and 72.3 ± 10.5% at 25 μM NEM. However, the rate was stimulated slightly by 18.3 ± 8.2% at 13 μM oligomycin. Transport was directly related to the concentration of reconstituted H⁺-ATPase and decreased 2.5-3.7 fold if the ATPase was heat-treated at 60 °C for 10 min before reconstitution. The transport appeared specific for trapped Fe with ¹⁴C-dextran (M.W.5000) being transported 7.7 ± 1.1% at 2.5 hours. Reconstituted mitochondrial cytochrome C was ineffective in transporting trapped components. When the ATPase was reconstituted into liposomes composed of PS:PE:PC (1:2:9), transport at 2.5 hours for ⁵⁹Fe³⁺ was 32.6%, for ⁵⁹Fe²⁺ 32.9%, and only 7.1 ± 1.7% for ¹⁴C-sucrose. These data support a role for bovine heart mitochondrial ATPase as an iron transporter when reconstituted into two different proteoliposomes system and support a more general role for H⁺-ATPases in iron transport.

M-Pos534

CHARACTERIZATION OF CHICKEN MUSCLE ECTO-Mg-ATPases ((James G. Stout and Terence L. Kirley)) Department of Pharmacology and Cell Biophysics, University of Cincinnati, Cincinnati, Ohio 45267-0575

The chicken ecto-Mg-ATPases are divalent cation-dependent, low abundance, high activity NTPases that are stimulated by lectins and hydrolyze extracellular NTPs. In this study, chicken ecto-Mg-ATPases were purified from gizzard smooth muscle and heart using a general method which included several ion exchange and lectin affinity chromatography steps that provide insight into characteristics of these enzymes. The solubilized and purified chicken gizzard enzyme is stimulated by Concanavalin A (Con A). Interestingly, solubilized chicken heart contains two peaks of Mg-ATPase activity with only the first peak being stimulated by Con A. Western blot analysis of the anion exchange purification stages with an antibody raised against truncated cadherin (T-cadherin) revealed a reactive band at 90 kDa presumed to be T-cadherin. However, for the Con A stimulated gizzard and heart enzymes, T-cadherin was separated from the Mg-ATPase activity by anion exchange chromatography, indicating that T-cadherin is not identical to the ecto-ATPase as has been proposed (ABB 303, 32-43 (1993)). Gizzard ecto-Mg-ATPase consists of a single, diffuse glycoprotein band at 66 kDa with a core protein of 53 kDa. Thus, the chicken ecto-ATPase is very similar to the rabbit ecto-ATPase (JBC 267, 11777-11782 (1992)). In addition, whole cells from gizzard and heart were isolated from 14 day chick embryos and evaluated for ecto-Mg-ATPase. (NIH AR38576, AR01841, HL07382).

M-Pos531

FUNCTION WITHIN TRANSMEMBRANE REGIONS OF THE H,K-ATPase ((E.C. Rabon, and K. Smillie)) Tulane Medical Center and VA New Orleans 70112

Various lines of evidence indicate that ligand binding influences the conformation of the H,K-ATPase. Several residues / domains important or essential for enzyme functions have been identified in the cytoplasmic and extracytoplasmic elements of this pump. To derive evidence of the functional importance of specific transmembrane domains of the H,K-ATPase we have labeled the membrane bound pump with either the hydrophobic thiol reagent, IANBD, or the hydrophobic carboxylic acid reagent, DCCD. Labeled, transmembrane domains obtained in the sedimented pellet following extensive trypsin digestion were resolved by SDS PAGE. K⁺-specific IANBD incorporation inhibited approximately 50% of the pNPPase activity in a monoexponential time course with k = .034 ± .005 min⁻¹ and placed the inhibitor within a region sensitive to the binding of ATP, Mg²⁺ and K⁺. IANBD fluorescence was localized exclusively to the M_r = 94 kDa α subunit of the H,K-ATPase and to a M_r = 7.8 kDa membrane-bound, peptide fragment with N terminal sequence, GTEP. This places IANBD within the M1/M2 transmembrane domain of the H,K-ATPase. Reaction with DCCD inactivated the H,K-ATPase and ⁸⁶Rb⁺ binding in a K⁺ protectable manner and incorporated [¹⁴C]-DCCD in an identical time course. Tryptic digestion in the presence and absence of K⁺ revealed that the majority of [¹⁴C]-DCCD was incorporated either into an M_r = 21 kDa or an M_r = 11 kDa peptide with identical N terminal sequence, LVNE. This places the majority of the [¹⁴C]-DCCD within the M7/M8 transmembrane loop. The reactivity of functionally important, hydrophobic residues in M1/M2 and M7/M8 transmembrane loops are conformationally sensitive, dependent upon the presence or absence of K⁺.

M-Pos533

THREE SEGMENTS OF THE *ESCHERICHIA COLI* ATP SYNTHASE γ SUBUNIT INTERACT TO MEDIATE COUPLING.

((Robert Nakamoto¹ and Masamitsu Futai²)) ¹Department of Molecular Physiology and Biological Physics, University of Virginia, Charlottesville, VA 22908 U.S.A., and ²Institute for Scientific and Industrial Research, Osaka University, Ibaraki, Osaka, 567 Japan.

The FoF₁ ATP synthase couples movement of protons across the membrane to synthesis or hydrolysis of ATP. We have used a mutagenesis approach to identify segments of the γ subunit involved in linking transport to catalysis. Substitution of γMet-23 with Arg or Lys caused extremely inefficient coupling (Shin et al., 1992, *J. Biol. Chem.* 267, 20835), and this perturbation was suppressed by several second-site mutations in the carboxyl-terminal region between γGln-269 and γVal-280 (Nakamoto et al., 1993, *J. Biol. Chem.* 268, 867). The suppression suggested that interactions between termini of the subunit are involved in the coupling mechanism. In this report, we further defined γ subunit interactions by focusing on two carboxyl-terminal substitutions, γGln-269 → Glu and γThr-273 → Val (both of which suppressed the effects of γLys-23 and were themselves deleterious). For γGlu-269 and γVal-273 mutants, several second-site suppressors in two regions were identified: γLys-18 to γGln-35, close to the original γLys-23 mutation, and γAla-236 to γMet-246, near the carboxyl-terminal region. Taken together, the suppressors define three segments of the γ subunit which interact to mediate energy coupling. These segments correspond to the three regions found conserved in known γ subunit sequences. Supported by the Ministry of Education, Japan, and the JSPS.

M-Pos535

Ca²⁺ AND Mg²⁺ TRANSPORT BY RAT LIVER ENDOPLASMIC RETICULUM AND MICROSOMAL VESICLES. ((A. Romani, C. Marfella and A. Scarpa)) Dept. Physiology and Biophysics, Case Western Reserve Univ., Cleveland, OH, 44106, USA.

Previous evidence from our laboratory suggests the involvement of liver endoplasmic reticulum (E.R.) during the cellular Mg²⁺ uptake observable under hormonal stimulation (i.e. vasopressin), possibly in exchange with reticular Ca²⁺. This phenomenon was further investigated by using digitonin-permeabilized hepatocytes or isolated microsomal vesicles. Permeabilized hepatocytes accumulated approx. 2 nmol Mg²⁺/mg protein, an amount equivalent to the quantity of reticular Ca²⁺ releasable by IP₃. This uptake was also observable under experimental conditions in which mitochondria were functionally inhibited by NaHg or cyanide. Microsomal vesicles were prepared in the absence (MS w/o Mg²⁺) or in the presence of 1 mM Mg²⁺ (MS w/ Mg²⁺) during the tissue homogenization and throughout the entire preparation. MS w/o Mg²⁺ accumulated approx. 25% less Ca²⁺ than MS prepared w/ Mg²⁺. This difference persisted also when Ca²⁺ trapping agents (i.e. Pi, G6Pi or oxalate) were used to enlarge the amount of Ca²⁺ accumulated into the vesicles. During the active Ca²⁺ accumulation a concomitant and equivalent Mg²⁺ release from MS w/ Mg²⁺ was observed, while no Mg²⁺ efflux occurred in MS w/o Mg²⁺. The presence of 200 μM vanadate or 200 nM thapsigargin in the incubation medium prevented both active Ca²⁺ uptake into and Mg²⁺ release from MS w/ Mg²⁺. On the other hand, when vanadate or thapsigargin were added after Ca²⁺ accumulation, a marked decrease in microsomal Ca²⁺ content and reaccumulation of Mg²⁺ were observed. These data suggest the existence, in the endoplasmic reticulum membrane, of a mechanism exchanging Ca²⁺ for Mg²⁺. This mechanism, which operates with a Mg/Ca exchange ratio of 1, may be important for the regulation of Ca²⁺ and Mg²⁺ cellular homeostasis and consequently a variety of cellular functions. (Supported by Grant N.I.H. HL 18708).

M-Pos536

SIMILAR INHIBITORY EFFECT OF HALOTHANE ON THE FUNCTION OF THE Ca^{2+} -ATPase FROM CEREBELLUM AND ERYTHROCYTES. ((Grazyna Roszczynska, Ludmila Zylinska, and Danuta Kosk-Kosicka), Johns Hopkins University, School of Medicine, Department of Anesthesiology, Baltimore, MD 21287.

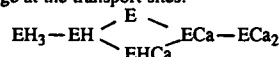
Recently we have demonstrated that volatile anesthetics inhibit activity of the Ca^{2+} -ATPase of human erythrocytes. We chose the enzyme as a model for studies of the mechanism of action of the anesthetics because it is an integral membrane protein and because it is solely responsible for Ca^{2+} transport in the cell thus fitting the proposed characteristics of a potential target for anesthetics in vivo. The inhibition is dose-dependent, reversible, involves hydrophobic interactions, and occurs at clinically relevant concentrations. Our present study compares the effect of halothane on the erythrocyte Ca^{2+} -ATPase with its effect on the synaptosomal plasma membrane Ca^{2+} -ATPase of rat cerebellum. We demonstrate that the inhibition pattern of the activity of the Ca^{2+} -ATPase from these two widely different tissues are very similar, as measured in parallel using either the two kinds of membranes or directly, the Ca^{2+} -ATPases purified from the two membranes. Half-maximal inhibition at 37°C is observed at 0.8 vol% (0.27 mM) halothane for the Ca^{2+} -ATPase activity in synaptosomal membranes and at 0.4 vol% in the purified Ca^{2+} -ATPase. It is plausible that impairment of this enzyme, instrumental in maintaining Ca^{2+} homeostasis in brain may be in fact related to anesthetic effects occurring in clinical anesthesia. (NIH GM 447130 and AHA 92010190)

M-Pos538

INTERACTION BETWEEN NUCLEOTIDE AND TRANSPORT SITES OF THE SARCOPLASMIC RETICULUM ATPase AS ILLUSTRATED BY Ca^{2+} BINDING IN THE PRESENCE OF NUCLEOTIDE.

((E. Mintz, V. Forge, M. Passafiume, A. Mata and F. Guillain)) SBPM and URA CNRS 1290, DBCM, CEN Saclay, 91191 Gif/Yvette, France. (Spon. by J.J. Lacapère)

The presence of excess ATP is known to enhance Ca^{2+} -ATPase activity, and among other effects, to accelerate the Ca^{2+} binding step. In a previous work, we have studied the Ca^{2+} binding step and its dependence on pH (Forge, Mintz & Guillain 1993, *J. Biol. Chem.* 268, 10953 and 10961). This has led us to a detailed description of the Ca^{2+} binding step as a $3\text{H}^+/2\text{Ca}^{2+}$ exchange at the transport sites:



Taking advantage of this description, we have studied the effect of ATP analogs on Ca^{2+} binding kinetics and equilibrium. At pH6, 0.3mM AMPPCP, AMPPNP, or ATP(γ -S) increase the affinity for Ca^{2+} and accelerate the Ca^{2+} binding kinetics. Conversely, at pH8, there is no effect neither on equilibrium nor on kinetics of Ca^{2+} binding. The effect of nucleotides was the same in the presence of 3mM Mg^{2+} . This is interpreted as if nucleotide binding at pH6 was inducing deprotonation of the Ca^{2+} deprived ATPase, switching to a species which binds Ca^{2+} faster and with a higher affinity, as observed at higher pH. As a consequence, a small difference is expected in the affinity for ATP between pH6 and pH8.

M-Pos540

SELECTIVE SPIN-LABELING OF SARCOPLASMIC RETICULUM CA-ATPASE: IMPLICATIONS REGARDING PHOSPHOLAMBAN REGULATION.

((S. Negash, L. Chen, D.J. Bigelow and T.C. Squier.)) Department of Biochemistry, University of Kansas, Lawrence, Kansas 66045.

We have synthesized a ^{14}C -radiolabeled maleimide spin label (MSL) in order to assess the specificity of labeling of the Ca-ATPase from both skeletal and cardiac sarcoplasmic reticulum (SR) membranes. Using ^{14}C -MSL, we have developed conditions for the selective labeling of the Ca-ATPase, allowing us to directly assess protein-protein interactions in native sarcoplasmic reticulum (SR) membranes through the use of spin-label ST-EPR measurements of the rotational dynamics of the Ca-ATPase. Spin-label EPR measurements of the rate of rotational diffusion of the Ca-ATPase in cardiac and skeletal muscle SR indicate that the Ca-ATPase from skeletal SR undergoes faster rotational motion than that observed in cardiac SR. The slower rotational mobility of the Ca-ATPase in cardiac SR membranes is attributed to direct interactions between the Ca-ATPase and phospholamban (PLN). Upon phosphorylation of PLN, the rotational mobility of the Ca-ATPase from cardiac SR is virtually identical to the Ca-ATPase from skeletal SR indicating a reduction in protein-protein interactions. We suggest that phospholamban directly regulates cardiac Ca-ATPase through changes in protein-protein associations.

M-Pos537

EFFECTS OF CALCIUM CHELATORS ON ^{45}Ca UPTAKE INTO RAT BRAIN MICROSOMES. ((J.E. Moore and R.F. Abercrombie)) Department of Physiology, Emory University, Atlanta, GA 30322.

Because calcium uptake into intracellular organelles is dependent upon free calcium concentration, many studies have used calcium chelators to hold free calcium constant. We examined whether chelators, including EGTA, BAPTA, and FLUO3, had any effect on the initial uptake rate or the total ^{45}Ca accumulated in rat brain microsomes. We isolated microsomes from whole brain and incubated them in an intracellular ionic media (pH 7.4, 37°C) which contained 3mM MgATP and various concentrations (10-1000 μM) EGTA or BAPTA or (10-100 μM) Fluo3. Uptake was examined over a time course of 10 seconds to 10 minutes. Free Ca was held constant at 0.6 μM , confirmed by calcium sensitive mini-electrodes. ATP-dependent calcium accumulation increased with time up to 10 minutes and was enhanced with increasing concentrations of chelator (free calcium was constant). In the presence of 10 and 100 μM chelator, calcium accumulation was elevated, respectively, 6-10 and 12-30 times over the same conditions without chelator. Initial rates and total accumulation were different for each of the three chelators. For example, in the presence of ~100 μM EGTA (0.6 μM free calcium), ^{45}Ca accumulation increased from 2.1 $\mu\text{mol/g}$ protein after 30 seconds to 8.9 $\mu\text{mol/g}$ protein after 10 minutes. In the presence of ~100 μM BAPTA (0.6 μM free calcium), calcium accumulation increased from 1.05 $\mu\text{mol/g}$ protein after 30 seconds to 4.4 $\mu\text{mol/g}$ protein after 10 minutes. Calcium uptake with Fluo3 was between that with EGTA and BAPTA. We conclude that mobile Ca chelators may facilitate ATP-dependent calcium transport. Supported by NIH NS-19194

M-Pos539

CONFOCAL CHARACTERIZATION OF CALCIUM UPTAKE IN SINGLE ISOLATED *XENOPUS* OOCYTE NUCLEI. ((L. Stehno-Bittel and D. E. Clapham)) Pharmacology Dept, Mayo School of Medicine, Rochester, MN 55009.

Calcium transients in single isolated nuclei from *Xenopus* oocytes were visualized using calcium-sensitive dyes; Fluo-3, Calcium green (unmodified and dextran forms) and Indo-1 (membrane permeant and impermeant forms). The nuclei were bathed in a mock intracellular solution with calcium clamped at 100, 200, 500 and 1000 nM concentrations using EGTA. Intra-nuclear calcium concentrations were similar to bath concentrations in the absence of ATP. However, when 1mM ATP was added to the bath (calcium-clamped at 100 or 200 nM) the intra-nuclear calcium rose to nearly μM levels as measured by Indo-2 ratioing. The high intra-nuclear calcium persisted in the presence of ATP, but was lost with the addition of the detergents to the bath. ATP-induced uptake of calcium was inhibited by prior exposure to CPA (5 μM , 90% inhibition), but only weakly inhibited by incubation in 1 μM thapsigargin (25% inhibition). Addition of ADP and the nonhydrolysable analogue of ATP (ATP γ S) did not induce nuclear calcium uptake. Thus, the nuclear membrane contains an ATP-dependent calcium uptake mechanism that increases calcium in the lumen of the nucleus.

M-Pos541

PROTEIN KINASE C CATALYZED PHOSPHORYLATION OF PLASMA MEMBRANE Ca^{2+} -ATPase FROM CEREBELLUM AND RED CELLS. ((Ludmila Žylinska and Danuta Kosk-Kosicka), Johns Hopkins University, School of Medicine, Department of Anesthesiology, Baltimore, MD 21287.

The plasma membrane Ca^{2+} -ATPase purified from two different tissues, rat cerebellum and human red blood cells, was phosphorylated by protein kinase C (PKC). The effect of different PKC activators including PS, PMA and DAG on regulation of the Ca^{2+} -ATPase by PKC was compared; Levels of ^{32}P incorporation into the Ca^{2+} -ATPase and the Ca^{2+} -ATPase activity were determined. At 500 μM free Ca^{2+} , with no other activator added, the ^{32}P incorporation was similar in the two enzymes. The effects of activators differed for the two Ca^{2+} -ATPases and depended on the presence of calmodulin. In the absence of calmodulin PMA was the most efficient activator: it increased phosphorylation levels in the Ca^{2+} -ATPase from cerebellum and red cell by 40% and 500%, respectively. In the presence of calmodulin high levels of phosphorylation were observed also with the other activators. The increase was most pronounced with PS/PMA and DAG/PS for the Ca^{2+} -ATPase from cerebellum, and with DAG and DAG/PS for the red cell enzyme. The PKC catalyzed phosphorylation resulted in changes in the Ca^{2+} -ATPase activity. Our observations suggest an intriguing possibility that PKC-dependent phosphorylation could be a regulatory mechanism of the plasma membrane Ca^{2+} -ATPase with tissue specific activator requirements. Supported by NIH GM 447130 and AHA 92010190.

M-Poe542

INACTIVATION OF SKELETAL MUSCLE SARCOPLASMIC RETICULUM Ca-ATPase INDUCED BY 2,2'-AZOBIS-(2-AMIDINOPROPANE) DIHYDROCHLORIDE (AAPH). ((Rosa Viner, Diana Bigelow, and Christian Schöneich)) Depts. of Biochemistry and Pharm. Chem., Univ. of Kansas, Lawrence, 66045.

Purified sarcoplasmic reticulum membranes from rabbit skeletal muscle were exposed to thermolabile, water-soluble free radical initiator AAPH. AAPH caused a time-dependent and biphasic inhibition of the Ca-ATPase activity. SDS-gel electrophoresis showed that in samples which were exposed to AAPH, the amount of monomeric and dimeric Ca-ATPase polypeptides in membranes decreased and the products of their oligomerization appear (mol. weight of these aggregates are more than 200 kDa). The loss of monomeric and dimeric species and the accumulation of oligomeric species correlated well with the extent of inactivation of the Ca-ATPase. We have not detected the appearance of any oxidant-induced peptide fragments. The formation of intramolecular Ca-ATPase cross-links is not connected with oxidation of the SH-groups of the enzyme to disulfides, but the azo-compound peroxyl radicals rapidly oxidize protein's tryptophans at a rate that is identical to that of inactivation. We suggest that the mechanism of Ca-ATPase inhibition induced by AAPH is oxidation of tryptophans, leading to the formation of intermolecular cross-links.

M-Poe544

THE AUTOINHIBITORY REGION OF THE PLASMA MEMBRANE Ca^{2+} PUMP IS LONGER THAN THE CALMODULIN-BINDING DOMAIN ((A. Enyedi, A.K. Verma, A.G. Filoteo and J.T. Penniston)) Department of Biochemistry and Molecular Biology, Mayo Foundation, Rochester, MN 55905

The plasma membrane Ca^{2+} pump activity is stimulated by direct interaction with calmodulin. Calmodulin binds to a regulatory domain (C domain) which is located near the carboxyl terminus of the enzyme. Utilizing a heterologous expression system for this pump in COS cells, the Ca^{2+} pumping activity of constructs containing various portions of the putative 28-residue C domain of hPMCA4b were compared. A mutant which lacked all 28 residues of the C domain and everything downstream from it, showed high activity and no response to calmodulin. As the length of the C domain in the constructs increased, the pump's activity decreased and the ability of calmodulin to stimulate the activity increased. The construct containing all 28 residues of the C domain restored all of the ability of the enzyme to bind calmodulin, but restored only half of the inhibition observed in the native enzyme in the absence of calmodulin. This indicates that the rest of the inhibitory properties reside further toward the carboxyl terminus. (Supported by NIH grant GM 28835.)

M-Poe546

EPIOTOPE LOCATION AND ISOENZYME SPECIFICITY OF THREE MONOCLONAL ANTIBODIES AGAINST THE PLASMA MEMBRANE CALCIUM PUMP ((A.J. Caride, A.G. Filoteo, A. Enyedi, and J.T. Penniston)) Mayo Foundation, Rochester, MN 55905

The monoclonal antibodies (Mabs) JA3, JA9 and 5F10, raised against the erythrocyte calcium pump, were used in many studies about the localization of the Ca pump and physiology of Ca transport. It has been shown (Adamo et al., JBC 267:14244, 1992) that JA3 reacted with an epitope located between aa. 1135-1204, JA9 with residues 17-75 and 5F10 with residues 724-783 (the numbers correspond to the aa. sequence of the isoform human 4b). In this work, we tested the reactivity of these Mabs against different synthetic peptides, 25 aa long, that covered the sequences mentioned above. By the pattern of reaction of these series of peptides with the antibodies, the epitope for JA3 can be mapped at aa. 1155-1180, the epitope for JA9 at aa. 51-75, and the epitope for 5F10 at aa. 714-738. By testing the reaction of these Mabs with peptides corresponding to the homologous regions of the different rat isoforms of the Ca pump it is shown that Mabs JA3 and JA9 reacted only with the peptides corresponding to the human 4 isoenzyme (4b in the case of JA3). On the contrary, Mab 5F10 bound to the peptides corresponding to all 4 rat isoforms. (Supported by NIH grant DK44902.)

M-Poe543

LABELING OF A PUTATIVE Mg^{2+} SITE ON THE SR Ca-ATPase GIVES EVIDENCE OF Ca^{2+} CONTROL OF THE Mg^{2+} SITE AFFINITY. ((Carol Coan, Pia Jakobs, Ji-Ying Ji, and Alexander J. Murphy)) Depts. of Physiology and Biochemistry, Univ. of the Pacific, San Francisco, CA 94115.

Following incubation with EDC [1-ethyl-3-(3-dimethylaminopropyl)carbodiimide], the sarcoplasmic reticulum Ca-ATPase loses activity and the ability to be phosphorylated by either Pi or ATP. 4 nmol of tempamine, or 14 nmol of pyridoxamine, per mg SR protein can be coupled to glu or asp side chains through the EDC reaction. Mg^{2+} protects against loss of activity, fully protects against tempamine labeling, and protects against approximately 4 nmol of pyridoxamine labeling. The Kd of a putative Mg^{2+} site can be estimated from the concentration of Mg^{2+} required for protection. In the absence of Ca^{2+} , this Kd (3 mM) is similar to the Kd for a Mg^{2+} that serves as a cofactor in phosphorylation by Pi. Ca^{2+} binding in the micromolar range has no discernable effect on the labeling or the loss in activity. However, the Kd for Mg^{2+} is lowered to 0.4 mM with Ca^{2+} present. Since Mg^{2+} is a cofactor in phosphorylation by either ATP or Pi, it is suggested that control of the Mg^{2+} binding site affinity is one means by which Ca^{2+} activates the enzyme. Supported by NIH Grants GM38073 and GM31083.

M-Poe545

INCREASED PROTEOLYTIC SUSCEPTIBILITY OF THE Ca-ATPase FROM AGED AND OXIDIZED SARCOPLASMIC RETICULUM. ((D.A. Ferrington, T.E. Jones, R. Viner, K. Thompson, & D.J. Bigelow)) Dept. of Biochemistry, Univ. of Ks., Lawrence, KS 66045

We have compared effects of aging and oxidation on the proteolytic susceptibility of the sarcoplasmic reticulum (SR) Ca-ATPase. *In vitro* oxidation of skeletal SR results in complete inactivation of the Ca-ATPase, which correlates with an increased rate and extent of tryptic susceptibility. Similarly, SR isolated from young (5 mo) and old (28 mo) Fischer strain 344 male rats shows different susceptibility to trypsin. SR from old animals subjected to mild tryptic digestion demonstrates a more rapid loss of Ca-ATPase activity in the first 10 minutes of digestion which correlates with a loss of intact 100 kD Ca-ATPase protein, suggesting increased accessibility of surface tryptic sites. Exhaustive tryptic digestion of SR isolated from old rats shows an increased rate of protein fragmentation, indicating age-related conformational changes of the overall protein structure. Although these conformational changes in native SR of old animals are not associated with decreased enzymatic activity of the Ca-ATPase, they may describe protein changes that occur when the organism experiences oxidative stress.

M-Poe547

PROTEIN AND LIPID DYNAMICS OF ASYMMETRICALLY RECONSTITUTED CA-ATPASE PROTEOLIPOSOMES. ((Qing Yao and Diana J. Bigelow)) Dept. of Biochemistry, Univ. of Kansas, Lawrence, Kansas 66045.

Affinity purified sarcoplasmic reticulum Ca-ATPase was reconstituted into egg phosphatidylcholine and egg phosphatidic acid (9:1) as described by Levy et al. [Levy, D., Gullik, A., Bluzat, A. & Rigaud, J.L., (1992) *Biochim. Biophys. Acta.* 1107, 283]. FITC binding stoichiometries indicate that 92-95% of reconstituted Ca-ATPase are in a right-side-out orientation. High molar lipid-to-protein ratios are accompanied by increased average lipid fluidity, as measured by stearic acid spin labels partitioned into the bilayer. Saturation-transfer EPR measurements of maleimide spin-labeled Ca-ATPase in reconstituted proteoliposomes demonstrate apparent correlation times of 180 μ s compared to 57 μ s in native SR, suggesting extensive self-association of reconstituted Ca-ATPase protein. We find that decreased protein mobility is accompanied by inhibition of enzymatic activity; calcium-dependent ATPase activity in reconstituted vesicles is only 80% that of native SR, despite the two-fold enrichment of the Ca-ATPase. However, this functional inhibition is completely reversed by solubilization with nonionic detergent.

M-Poe548

Measurements of ATP binding on the large cytoplasmic loop of the sarcoplasmic reticulum Ca^{2+} -ATPase over-expressed in *E. coli*

(Marie-Jo Moutin*, Martine Cuillel*, Catherine Rapin*, Roger Miras*, Marielle Anger**, Anne-Marie Lompré**, and Yves Dupont*)

(*) Laboratoire de Biophysique Moléculaire et Cellulaire, URA 520 du CNRS, CEA Grenoble, France. (**) INSERM U-275-LOA, ENSTA Ecole Polytechnique, Centre de l'Yvette, Palaiseau, France.

The large cytoplasmic loop of the sarcoplasmic reticulum Ca^{2+} -ATPase (LCL), situated between Lys₃₂₉ and Phe₇₄₀, is believed to contain its ATP binding locus. A cDNA fragment coding for this amino-acids sequence was generated in vitro and cloned in vector pQE8. This allowed the over-expression in *E. coli* of the Ca^{2+} -ATPase domain fused with a cluster of six histidines at its N terminal. The fusion protein produced in an insoluble form within bacteria was solubilized in 4 M urea, purified on immobilised Ni^{2+} and then renatured by elimination of urea. More than 4 mg of purified renatured fusion protein was obtained from 500 ml of culture.

ATP binding on the refolded protein was demonstrated by two methods: (1) detection of ATP-induced intrinsic fluorescence change and (2) binding of the fluorescent ATP analogue 2',3'-O-(2,4,6-trinitrophenyl)adenosine-5'-triphosphate (TNP-ATP) and its chase by ATP. It is shown that the LCL protein has one single TNP-ATP binding site having a dissociation constant (Kd) of 1.6-1.9 μM . Both methods yielded a Kd for ATP around 200 μM . Binding of other nucleotides was detected with a sequence of Kd identical to that found for native Ca^{2+} -ATPase: ATP < ADP < GTP < AMP < ITP. A Mg^{2+} binding site was also found on the LCL protein (Kd = 100 μM at pH 7.2). The fluorescence of bound TNP-ATP was found to be highly dependent on Mg^{2+} binding on this site.

M-Poe550

Amino Acids Lys-Asp-Asp-Lys400 in the Cardiac Ca^{2+} -ATPase (SERCA2) are critical for Functional Association with Phospholamban.

(Toshihiko Toyofuku*, Michihiko Tada*, and David H. MacLennan*)

*Charles H. Best Institute, University of Toronto, Toronto M5G 1L6 CANADA and * Department of Medicine and Pathophysiology, Osaka University School of Medicine, Suita, Osaka 565, JAPAN

Phospholamban inhibits the Ca^{2+} -transport activity of SERCA1 and SERCA2 isoforms of the Ca^{2+} -ATPase, but not SERCA3. Studies of a series of chimeras between SERCA2 and SERCA3, coexpressed with phospholamban, showed that amino acids 336 to 412 in the phosphorylation domain and amino acids 467-762 in the nucleotide binding/hinge domain of SERCA2 are required for phospholamban interaction (Toyofuku, T., Kurzydowski, K., Tada, M., and MacLennan, D.H. (1993) J. Biol. Chem. 268, 2809-2815). When a series of mutations were made in SERCA2 between amino acids 336 and 412 and mutants were coexpressed with phospholamban in HEK-293 cells, interaction with phospholamban was disrupted for mutants K397Q plus K400Q, K397E plus K400E, or D398R plus D399R. Single amino acid changes K397Q, D398G, D399E or K400Q in the sequence KDDK400 of SERCA2 did not affect phospholamban interaction. The chimera CH10, in which the nucleotide binding/hinge domain of SERCA2 was inserted into SERCA3, did not interact with phospholamban. When the sequence GGEQ400 was mutated to KDDK400 in CH10, functional interaction with phospholamban was observed. These results suggest that the sequence KDDK400 makes up a critical site for phospholamban interaction with the Ca^{2+} -ATPase. (Supported by the Heart & Stroke Foundation of Ontario and the Human Frontier Science Program Organization).

M-Poe552

HIGH SENSITIVITY TO SITE DIRECTED MUTAGENESIS OF THE PEPTIDE SEGMENT CONNECTING PHOSPHORYLATION AND Ca^{2+} BINDING DOMAINS IN THE Ca^{2+} TRANSPORT ATPase.

((Ziyu Zhang, Carlota Sumbilla, David Lewis and Giuseppe Inesi)) Department of Biological Chemistry, School of Medicine, University of Maryland, Baltimore, Maryland 21201

The peptide segment intervening between catalytic (extramembraneous) and calcium binding (transmembrane) domains retains a high degree of homology in cation transport ATPases, indicating that structural integrity of this region is prominently required for function. Nine residues in this segment (Leu³²¹, Lys³²⁹, Asn³³⁰, Val³³³, Arg³³⁴, Leu³³⁶, Pro³³⁷, Val³³⁹ and Glu³⁴⁰) of the sarcoplasmic reticulum (SERCA 1) ATPase were individually mutated to Ala. The mutated proteins were recovered in the microsomal fraction of COS-1 cells following transient expression, and exhibited inhibition of Ca^{2+} uptake and ATPase hydrolytic activity, while forming normal levels of phosphorylated intermediate. Mutation of Glu³⁴⁰ to Gln (rather than to Ala) was much less effective, suggesting that the functional consequence of the mutation is related to structural perturbation, rather than loss of the acidic side chain. The high sensitivity of this peptide segment to single mutations suggests that its stringent structural integrity is required for functional linkage of the phosphorylation and Ca^{2+} binding domains. This finding is likely to apply to other cation transport ATPases. (NIH and AHA supported).

M-Poe549

FUNCTIONAL ROLES OF AMINO ACIDS IN TRANSMEMBRANE SEQUENCES M5 AND M6 OF SERCA1. ((William J. Rice and David H. MacLennan)) Banting and Best Department of Medical Research, University of Toronto, Toronto Canada M5G 1L6

The Ca^{2+} ATPase of skeletal muscle sarcoplasmic reticulum (SERCA1) has been extensively mutagenized. Six residues located in transmembrane domains M4, M5, M6, and M8 have been implicated in Ca^{2+} binding. A study in which all residues in the M4 domain were singly mutated revealed the presence of a patch that was extremely sensitive to substitution. Mutation of these residues affected Ca^{2+} binding, Ca^{2+} affinity and ability to undergo conformational changes. These studies have been extended to domains M5 and M6. Domain M6 appears to contain a patch of residues located on one side of the helix that, when mutated, result in decreased Ca^{2+} affinity. In particular, mutant L807A has a Ca^{2+} affinity 10-fold lower than that of the wild type enzyme. The M5 domain contains a set of residues extending from Leu⁷⁶⁴ to Glu⁷⁷¹ that is also involved in Ca^{2+} binding or affinity. However, they do not form a patch on one side of the helix, but span the entire helical wheel. These are followed by a series of four residues insensitive to mutation, and finally by residue Ala⁷⁷⁹, which, when mutated to Leu, results in a 10-fold decrease in Ca^{2+} affinity. Comprehensive mutagenesis of transmembrane sequences should assist in the modeling of the Ca^{2+} binding domain. (Supported by National Institutes of Health, U.S.A.)

M-Poe551

A pK CHANGE OF ACIDIC RESIDUES CONTRIBUTES TO CATION TRANSLLOCATION BY THE SARCOPLASMIC RETICULUM Ca^{2+} ATPase ((X. Yu, L. Hao, G. Inesi)) Department of Biological Chemistry, University of Maryland at Baltimore School of Medicine, Baltimore, MD 21201 (spon. by K.D. Collins)

Proteoliposomal vesicles reconstituted with sarcoplasmic reticulum ATPase and exogenous lipids were used to demonstrate ATP dependent Ca^{2+} transport into the lumen of the proteoliposomes and H^{+} ejection from the lumen, as well as net charge displacement by Ca^{2+} . We have now studied the effect of luminal and (extravesicular) medium pH variations on the countertransport ratios of H^{+} and Ca^{2+} . We found that when luminal pH is set at 6.0, and medium pH at 7.0 or 8.0, the $\text{H}^{+}/\text{Ca}^{2+}$ ratio of the initial velocities is approximately 1. If medium pH is lowered to 6.0, however, the $\text{H}^{+}/\text{Ca}^{2+}$ ratio is only 0.5. Therefore, the pK of the residue(s) releasing H^{+} into the medium is approximately 6.0, and nearly full H^{+} dissociation is obtained at medium pH 7.0. If medium pH is then set at 7.0, the $\text{H}^{+}/\text{Ca}^{2+}$ ratio is 1 at luminal pH 6.0, 0.8 at luminal pH 7.0, and 0.6 at luminal pH 8.0. Therefore, the pK of residues binding luminal H^{+} is approximately 8.0, and nearly full H^{+} association is obtained at luminal pH 7.0. Assuming that the same acidic residues are involved in H^{+} and Ca^{2+} countertransport, our findings suggest a higher affinity for H^{+} in their luminal, as compared to outward orientation. This change, occurring in the opposite direction to Ca^{2+} affinity, may be produced by minor structural changes linked to catalytic events, and may promote cation exchange and inward Ca^{2+} displacement. A calculation of voltage development related to initial rates of charge transfer ($dV/dt = (dQ/dt)/C_m$) will be presented as a corrective replacement of a previous steady state calculation. (supported by NIH and Am. Heart Ass.)

M-Poe553

BEHAVIOR OF N-ACYLATED DAUNORUBICINS IN MULTI-DRUG RESISTANT AND PARENTAL CANCER CELLS.

((A. Aszalos, P.S. Pine, J.L. Weaver, P.V. Schoenlein, M.M. Gottesman and G. Szabo, Jr.)) Food and Drug Administration, CDER, Div of Research and Testing, Washington, D.C. 20204, Laboratory of Cell Biology, NCI, NIH, Bethesda, MD, and Medical School of Debrecen, Debrecen, Hungary. (Spon. by J. Reilly)

The behavior of daunorubicin and N-acylated daunorubicins was studied in parental and MDR1 gene transfected cell lines. For this purpose a flow cytometric method was employed. Suspension grown L1210 and L5178 lymphoma cells and the adherently grown NIH3T3 and the FEM-X melanoma cells were used. We found that N-acylated daunorubicins accumulate in parental and MDR1 gene transfected cells equally. We concluded that N-acylated daunorubicins are not substrates of the MDR1 pump. These compounds have an equal antiproliferative effect in parental and MDR1 gene transfected cells, unlike the parent compound. However their ED₅₀ values are 2 to 10 times higher than that of daunorubicin in the MDR gene transfected cells of the above mentioned cell lines. Confocal microscopic studies revealed differences in intracellular distribution. Daunorubicin fluorescence appeared more punctate with a peri- and intra-nuclear localization, while the N-dodecanoyl derivative appeared to have a more diffuse cytoplasmic distribution.

M-Poe554

OVEREXPRESSION OF μ MDR 1 PROTEIN INHIBITS Na^+ -INDEPENDENT $\text{Cl}^-/\text{HCO}_3^-$ EXCHANGE IN TRANSFECTED CHINESE HAMSTER OVARY CELLS (John Gately Luz, Li-Yong Wei, Subham Basu & Paul D. Roepe) Program in Molecular Pharmacology & Therapeutics, Memorial Sloan-Kettering Cancer Center and Graduate School of Medical Sciences Cornell University 1275 York Avenue, New York, New York 10021.

We have measured intracellular pH (pH_i) for multidrug resistant (MDR) cell lines constructed by transfecting LR73 fibroblasts with mutant and wild type murine MDR 1 genes. Plasma membrane electrical potential ($\Delta\psi$) has also been measured by the K^+ /valinomycin null point titration method using the ratiometric probe di-4-ANEPPS. Both the untransfected, parental cell line and a cell line expressing substantial mutant MDR 1 protein (K432R/K1074R) that is unable to confer the MDR phenotype are found to have $\Delta\psi \approx -40 (\pm 5)$ mV and $\text{pH}_i \approx 7.16 (\pm 0.03)$ units. In contrast, MDR cell lines constructed by transfecting wild type μ MDR 1 cDNA are found to exhibit $\Delta\psi$ 15 - 19 mV lower and pH_i from 0.13 to 0.34 units higher. Northern and western blot analyses confirm the substantial overexpression of the μ MDR genes and proteins in these lines, as well as the mild overexpression of endogenous hamster pGP mRNA in some lines. In general agreement with previous mass cell population studies that examined myeloma cells overexpressing hu MDR 1 protein (Roepe, P.D. *et al.*, *Biochemistry* in the press) we find that the overexpression of wild type μ MDR 1 protein inhibits Cl^- and HCO_3^- dependent pH_i homeostasis. Via single cell photometry studies we now conclude that this is due to specific inhibition of Na^+ - independent $\text{Cl}^-/\text{HCO}_3^-$ exchange (strict anion exchange or AE). Decreased AE activity is not due to decreased expression of the exchanger. In fact, again similar to previous work we find increased levels of AE mRNA in some MDR cell lines. Several models that explain these data that are also consistent with the known physiology of cells that endogenously express MDR protein are suggested. These data are consistent with a model for MDR protein function wherein overexpression of the protein decreases $\Delta\psi$ and/or elevates pH_i via Cl^- and HCO_3^- dependent mechanisms.

Supported by grants from the Raymond & Beverly Sackler Foundation, the Society of Sloan-Kettering, and a Cancer Center Support Grant (NCIP30CA08748). PDR is a Sackler Scholar at MSKCC.

M-Poe555

DETERGENT-MEDIATED SOLUBILIZATION OF P-GP CONTAINING MEMBRANES FROM MULTIDRUG RESISTANT CELLS

((M. Garrigos and S. Orlowski)) SBPM, DBCM/CEA, CE Saclay, F-91191 Gif/Yvette Cédex, France (Spon. by M. le Maire)

Overexpression of the glycoprotein P-gp in plasma membrane of tumor cells is responsible for their resistance to a large number of structurally unrelated cytotoxic drugs. The resistance results from a hyperflux of the drugs out of the cells and seems to be related to an ATP-dependent transport via the P-gp. To confirm this last point, it is necessary to reconstitute purified P-gp into liposomes. To this aim, a preliminary step is detergent-mediated membrane solubilization. We have used vesicles of purified total membranes from Chinese Hamster lung fibroblasts highly resistant to actinomycin D (DC-3F/ADX) to compare the efficiency in preserving P-gp ATPase activity of the following detergents: CHAPS, deoxycholate, C12E8, Triton X100, octylglucoside and dodecylmaltoside. Solubilization was conducted in PBS buffer $\text{pH}=7.5$, 20°C , with successive additions of detergent over a concentration range covering three decades, and monitored using both light scattering and sedimentation experiments. For all six detergents tested, P-gp ATPase activity decreases monotonously for increasing but still non-solubilizing detergent concentrations, and only CHAPS, at solubilization, is able to restore P-gp ATPase activity to its initial value. In all cases ATPase activation by verapamil is lost. Size exclusion liquid chromatography on detergent equilibrated TSK SW 3000 column shows that after a centrifugation at $100,000 \times g$ for 1 h the supernatant of CHAPS solubilized membranes contains P-gp mainly in an aggregated state, but still displaying ATPase activity.

FUNCTIONAL IMAGING OF THE BRAIN

Tu-AM-Sym1-1

COGNITIVE NEUROPHYSIOLOGY OF THE MOTOR CORTEX: STUDIES WITH SINGLE CELL RECORDINGS IN THE MONKEY. (A.P. Georgopoulos). Brain Sciences Center, Veterans Affairs Medical Center, Minneapolis, MN 55417.

Some principles underlying the representation and processing of directional information in the motor cortex will be discussed in this presentation. Large populations of neurons in motor cortex are engaged with reaching movements. This engagement is fairly early, starting approximately 60 ms following target onset. The intensity of cell discharge is modulated with the direction of reaching. Typically, the firing rate is a sinusoidal function of the direction. An unambiguous, distributed code for direction exists in neuronal populations in the motor cortex. The outcome of this population code can be visualized as a vector that points in the direction of the upcoming movement ("neuronal population vector"). The neuronal population vector has the following properties: it is an accurate and robust predictor of direction; it is resistant to cell loss; it can be estimated reliably from about 100-150 cells; it predicts well the direction during the reaction time, well before the motor output begins; it predicts the direction of reaching during an instructed delay period, in the absence of immediate motor output; and it predicts the direction of reaching during reaching in memorized directions, that is in the absence of a target. Finally, when a mental transformation is required for the generation of a reaching movement in a different direction from a reference direction, the population vector can provide useful information concerning the nature of the cognitive process by which the required transformation is achieved (Georgopoulos *et al.*: Mental rotation of the neuronal population vector. *Science* 243:234-236, 1989).

Tu-AM-Sym1-3

FUNCTIONAL MAPPING OF THE HUMAN BRAIN WITH POSITRON TOMOGRAPHY ((RSJ Frackowiak)) MRC Cyclotron Unit, Hammersmith Hospital, London W12 0HS, UK

Positron emission tomography is a radiotracer based technique which capitalises on back projection reconstruction algorithms to provide quantitative distributions of cerebral perfusion in the human brain non-invasively in life. Measurements of the distribution of perfusion can be recorded in various experimental and control states and comparisons can be made between them. Local cerebral perfusion is an index of local synaptic firing and hence perfusion mapping provides a means of understanding the anatomical substrate of various cortical and subcortical functions. The lecture will illustrate the principles of the technique and the information that can be obtained by reference to studies in the visual system.

Reference

Zeki S, Watson JDG, Lueck CJ, Friston KJ, Kennard C, Frackowiak RSJ. *J Neurosci* 1991;11:641-649.

Watson JDG, Myers R, Frackowiak RSJ, Hajnal V, Woods RP, Mazziotta JC, Shipp S, Zeki S. *Cereb Cortex* 1993;3:79-94.

Tu-AM-Sym1-2

MAGNETIC SOURCE IMAGING OF HUMAN BRAIN FUNCTIONS. ((S.J. Williamson)) Neuromagnetism Laboratory, Department of Physics and Center for Neural Science, New York University, New York, NY 10003.

The advent of large arrays of superconducting detectors now makes it possible to characterize the spatio-temporal dynamics of neural activity of the human brain from measurements of the magnetic field pattern near the scalp. The wide-band response of these sensors provides millisecond resolution in quantitatively defining the strength of local activity in the cerebral cortex. Our studies of two regions in the auditory cortex separated by only 1 cm reveal different dynamical features in primary and association areas which characterize distinct properties of sensory memories. These non-invasive 'physiological' studies of neural activity accurately predict the lifetime of auditory sensory memory (echoic memory) for individual human subjects. While the magnetic inverse problem provides no unique solution, it is nevertheless possible to obtain best estimates for the spatial distribution of intracellular electric currents. Such a magnetic source image (MSI) can account for the sources of magnetic field power, as well as the covariance between sources at different locations. Consequently, the magnetic observation of localized suppression of spontaneous rhythms, such as those in the alpha bandwidth, can be interpreted as desynchronization of cortical activity in specific anatomical areas, as when they become engaged in a sensory or cognitive task. By these methods, the rapid response of magnetic sensors can be exploited to characterize the fast-paced evolution of neural activity in various regions of the brain.

Tu-AM-Sym1-4

FUNCTIONAL BRAIN MAPPING WITH MAGNETIC RESONANCE IMAGING: RECENT DEVELOPMENTS AND ACCOMPLISHMENTS (Kamil Ugurbil, University of Minnesota, Center for Magnetic Resonance Research, Minneapolis, MN)

The study of the human brain requires methods of delineating regions of neuronal activity during performance of various tasks. A new magnetic resonance imaging (MRI) method has been shown to provide functional maps of the human brain using BOLD (Blood Oxygen Level Dependent) contrast. BOLD has its origin in the magnetic properties of hemoglobin and was first observed at high magnetic fields (Ogawa, *et al.*: (1990) *Magn. Reson. Med.* 14:68). Functional imaging with MRI is based on BOLD effect and the hemodynamic and metabolic response of the brain to increased neuronal activity.

Functional MRI has already been utilized to study sensory stimulation, motor task, and cognitive processes in humans. In this lecture, the present accomplishments, the potential and the limitations of the BOLD MRI functional imaging will be reviewed and discussed.